WIRELESS ENGINEER

Vol. XXVI MAY 1949 No. 308

The Radio Research Board

FOR many years past, *Wireless Engineer* has frequently published articles in which the authors make acknowledgments to the Radio Research Board and the Department of Scientific and Industrial Research; and we have sometimes wondered to what extent the scope and functions of these bodies are known to our readers. In view of the announcement over a year ago of the setting up of a new and enlarged Radio Research Organization under the above Department, the time would seem to be opportune for a review of the activities pursued by this organization.

The Department of Scientific and Industrial Research, usually referred to by the initials D.S.I.R., was established during the first World War to promote and organize scientific research, with a view especially to its application to trade and industry. The permanent head of D.S.I.R. is its Secretary, who for the past ten years has been Sir Edward Appleton, G.B.E., K.C.B., F.R.S.; he has been recently succeeded by Sir Ben Lockspeiser, F.R.S., M.A. With the exception of medicine and agriculture, the Department embraces in its scope all branches of natural science and their application to industrial processes. Its activities fall under three main headings:—(a) research in the national interest for the benefit of the community as a whole and to meet the requirements of Government Departments; (b) the encouragement of research and the application of scientific knowledge in industry; and (c) the encouragement of fundamental research at universities and elsewhere, and the maintenance of an adequate supply of trained research workers for laboratories of all kinds.

To provide for the discharge of these functions in the radio field, the Radio Research Board was established in 1920 to advise the D.S.I.R. on the nature and scope of a programme of research work of a fundamental nature in directions where it was lacking and where it would be likely to lead to useful applications. In the first years of its existence this programme of work was carried out partly at the National Physical Laboratory on fundamental measurements and standards, partly at special research stations established by the D.S.I.R. at Aldershot for investigating the nature and origin of atmospherics, and at Slough for studying radio direction finding, and partly by materially assisting certain lines of research at universities; and notably the classical work of Professor (now Sir Edward) Appleton and his colleagues on the investigation of the ionosphere and the propagation of radio waves. In 1933 a new Radio Division of the National Physical Laboratory was formed, with Mr. (now Sir Robert) Watson Watt as Superintendent, to unify the D.S.I.R. activities in radio, and simplify the task of planning and conducting the programme of research.

A few years later, a portion of this programme led to the first demonstrations of the possibilities of radiolocation, or radar as it is now called, and Mr. Watson Watt and a number of his colleagues left the D.S.I.R. to form a new research station at Bawdsey, which was the forerunner of the present Telecommunications Research Establishment. Throughout the second World War, Dr. R. L. Smith-Rose was Superintendent of the Radio Division of the National Physical Laboratory, which oriented its programme of research towards the particular needs of the Service

Departments and the sections of industry working for those Departments. Following a consideration of its post-war programme by the Radio Research Board, the D.S.I.R. in January 1948 appointed Dr. Smith-Rose to the new post of Director of Radio Research, to take charge of all the radio-research work of the Department, for which a new station will eventually be established.

While the constitution of the Radio Research Board has varied slightly from time to time, its members have always included representatives at the highest level of those Government Departments with an intimate interest in radio applications, and of the British Broadcasting Corporation together with some independent members, who may be connected with universities or with industrial organizations. The members of the Radio Research Board have all been eminent personages in radio science or the radio-engineering profession. Several are Fellows of the Royal Society, many have served as Chairmen of the Radio Section of the Institution of Electrical Engineers, while some have occupied the presidential chair of the Institution. The present chairman of the Radio Research Board is Col. Sir Stanley Angwin, K.B.E., D.S.O., M.C., T.D., Chairman of Cable & Wireless Ltd., and formerly Engineer-in-Chief of the Post Office. To assist the Board in its work a number of expert technical committees are formed from time to time; and while these are comprised in much the same way as the Board, their members are selected for their special knowledge and experience in the field of the committee on which they serve. The committees of the Board now in operation deal with the following subjects, which indicate the scope of the programme being pursued at present: the propagation of radio waves along the ground, through the troposphere and through the ionosphere; radio direction-finding; radio navigational aids; radio noise; measurements and standards; and materials for radio purposes. It will be noticed that in these subjects for research the emphasis is placed on seeking knowledge on the characteristics of waves over the entire radio spectrum and on some special techniques, rather than on the development of terminal equipment for various applications. This is a deliberate choice, since so many departments and industrial organizations are considered to be in a position to develop apparatus, whether of a sending, receiving or other type, specifically for their own requirements.

By and large, and except under conditions of wartime restrictions, the results of all the work carried out under the auspices of the Radio Research Board are published in papers presented before one or other of the scientific societies or engineering institutions, or in technical periodicals such as *Wireless Engineer*. Some of the material, including especially surveys of progress in various fields of radio knowledge, is published in official reports issued through H.M. Stationery Office. Apart from the research and investigation work conducted under its auspices, the Radio Research Board has organized and maintained for the past twenty years a service supplying a comprehensive series of abstracts and references which are published monthly in *Wireless Engineer*. These abstracts are unique in radio technical literature, and are greatly appreciated by radio engineers and research workers in all parts of the world. Their availability to the English reading public has been greatly extended by their complete reproduction by arrangement with us in the *Proceedings of the Institute of Radio Engineers* (New York) since June 1946.

It will be fitting to conclude this Editorial with a quotation from a speech made in 1943 on "Radio Research and Production, Before, During and After the War" by Mr. G. M. Garro-Jones (now Lord Trefgarne) who was then Parliamentary Secretary to the Ministry of Production.

> "In the decade 1925-35, the State contribution came through the Radio Research Board of the Department of Scientific and Industrial Research in full activity on a programme of work which largely centred on the effects of atmospheric processes in radio. The Board and the National Physical Laboratory also did great things in an active programme of measurements and standards work. The constitution of the Board and its committees, and the conduct of parts of the work in university laboratories maintained the essential linkage between radio research and the universities: . . . Radiolocation, by far the most important national asset ever to emerge from the National Physical Laboratory, was a natural but not inevitable synthesis of techniques developed within the Radio Research Board's programme. It revivified the laboratories of the Defence Services."

With the expanded programme of the Board now being inaugurated, and with the closer contact with industry now projected, we may look forward with interest to further fruitful results of fundamental investigations in radio phenomena.

GRAPHICAL ANALYSIS OF DIODE CIRCUITS

By G. L. Hamburger, Dipl.-Ing., A.M.I.E.E., M.Brit.I.R.E.

(Engineering Division, Central Rediffusion Services Ltd.)

LARGE-SIGNAL diode theory is a typical example of the frequent superiority of an engineering approach over a rigorous mathematical treatment. By superiority is meant in this case a quick, simple and comprehensive solution compared with a disproportionately elaborate mathematical procedure necessary to obtain any results at all. It should be kept in mind that it is nearly always the primary object of the designer of electronic circuits to obtain a qualitative picture of the manner in which they behave, and to predict the approximate value of the quantities involved. The knowledge of precise values is usually of lesser interest since it is easy enough to make a narrow adjustment in the practical circuit, quite apart from the fact that the circuit components themselves are rarely more accurate than plus or minus ten per cent. Assumptions have usually to be made in either case so that the results of an analysis have to be carefully applied to practice.

A case which presents itself frequently, and in various modifications, is that in which the grid of a triode or pentode takes grid current. The input is usually coupled to the grid (or the diode) by means of a capacitor ; a certain amount of rectification takes place, and the question arises as to what distortion of wave shape and what amount of rectification will take place. What is the mechanism of both ?

1. Basic Diode Circuit

The fundamental circuit which is to be analysed is shown in Fig. 1 (a), and its equivalent modifications in (b) and (c). The source voltage $v(t)$ is an alternating e.m.f. of arbitrary shape ; R_i is the internal source resistance ; C is the coupling capacitance which is assumed to be so big that is impedance at the fundamental frequency of v is negligible compared with all other impedances involved ; R_L is the leak resistance. The diode resistance r_D is assumed to be constant in the pass range and infinite for negative diode voltages.

Only the quasi-stationary state is to be analysed ; i.e., the e.m.f. is assumed to be truly periodic.

An arbitrary periodic e.m.f. is chosen and plotted in Fig. 2 as curve P_1 against earth potential. The voltage appearing on the other side of the capacitor [viz., the voltage P_2 to earth in Fig. 1 (c)] must be a precise replica of P_1 since there is no alternating voltage drop across C. However, since rectification is bound to take place in the presence of an unbiased diode, there will be a steady potential across the capacitor. This steady potential $V_0 = P_1 - P_2$. It follows that P_2 is the original e.m.f. P_1 shifted by the constant amount of rectification V_0 into more negative regions.

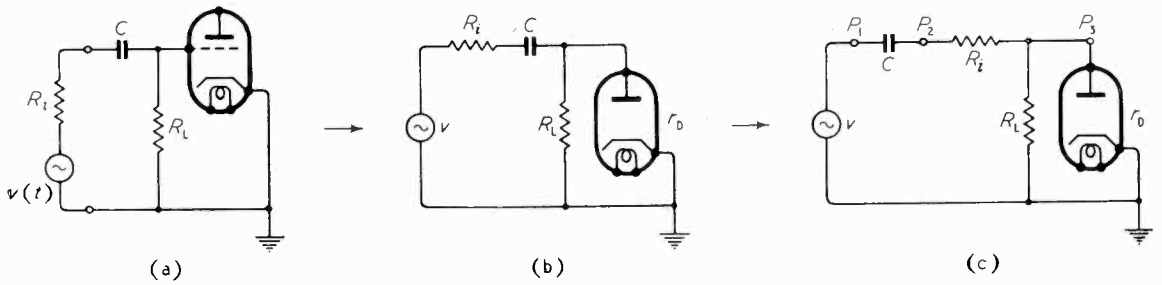

Fig. 1. *The circuit to be analysed is shown at (a) and its equivalents at (b) and (c).*

Finally the fact that for a quasi-stationary state the sum total of the current flowing into and out of the capacitor, say at P_2, Fig. 1 (c), must be zero will enable us to define the exact amount of rectification taking place. It can be seen from Fig. 2 that between the instants t_0 and t_1, the voltage at P_2 is positive with respect to earth and the cathode of the diode, and that between the instants t_1 and t_2 it is negative.

MS accepted by the Editor, February, 1948.

Therefore the diode takes current only between t_0 and t_1, and can be replaced by a resistance r_D. Hence

$$Q_1 = \int_{t_0}^{t_1} \frac{(v - V_0)dt}{R_i + \frac{R_L r_D}{R_L + r_D}} \quad .. \quad .. \quad .. \quad (1)$$

is the charge accumulated in the capacitor between t_0 and t_1, and

$$Q_2 = \int_{t_1}^{t_2} \frac{(v - V_0)\,dt}{R_i + R_L} \quad .. \quad .. \quad .. \quad (2)$$

is the charge that leaks away again between t_1

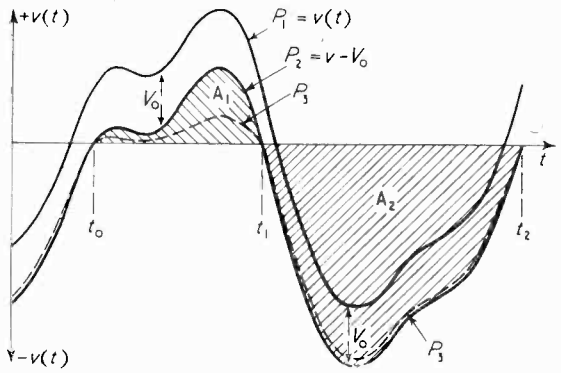

Fig. 2. *Curve P_1 represents an arbitrary input wave and P_2 indicates the grid-cathode voltage of the valve, the difference V_0 being the steady rectified voltage across C. P_3 shows the wave flattened during the conductive period of the diode.*

and t_2 when the diode is non-conductive. By putting

$$Q_1 = Q_2 \quad .. \quad .. \quad .. \quad .. \quad .. \quad (3)$$

the quasi-stationary state is fully defined. The integral equation determines the instants t_0, t_1 and t_2, and from them the rectified voltage V_0 can be evaluated.

Unfortunately, however, such integral equations can only be solved in very special cases. Even in the simplest case of a pure sinusoidal e.m.f. they lead to transcendental equations which can only be solved graphically. One such example is shown in the appendix, and though exact, the process is lengthy and not very edifying since one somehow loses touch with the circuit itself.

Nevertheless equations (1) and (2) suggest a direct graphical solution which, though only approximate, indicates the trend of the behaviour of the circuit.

From equations (1) and (2)

$$Q_1 = \frac{1}{R_i + \frac{R_L r_D}{R_L + r_D}} \int_{t_0}^{t_1} (v - V_0)\,dt = g_1 \int_{t_0}^{t_1} (v - V_0)\,dt = g_1 A_1 \quad .. \quad .. \quad .. \quad (4)$$

and $Q_2 = \frac{1}{R_i + R_L} \int_{t_1}^{t_2} (v - V_0)\,dt =$

$$g_2 \int_{t_1}^{t_2} (v - V_0)\,dt = g_2 A_2 \quad .. \quad (5)$$

where $g_1 = \frac{1}{R_i + \frac{R_L r_D}{R_L + r_D}}$,

and $g_2 = \frac{1}{R_i + R_L}$

are constant factors dependent on the three resistances R_i, R_L and r_D. In the present case g_1 is greater than g_2. The integrals A_1 and A_2 are then simply the shaded areas in Fig. 2.

2. Graphical Solution

Thus the method of arriving at the amount of rectification V_0 taking place for an arbitrary periodic e.m.f. impressed upon the diode circuit is simply this: plot a little more than one cycle of the e.m.f. on graph paper (Fig. 3), and draw a line parallel to the time axis such that it divides the curve into equal positive and negative areas within one complete cycle. Then find another horizontal line dividing the curve such that all

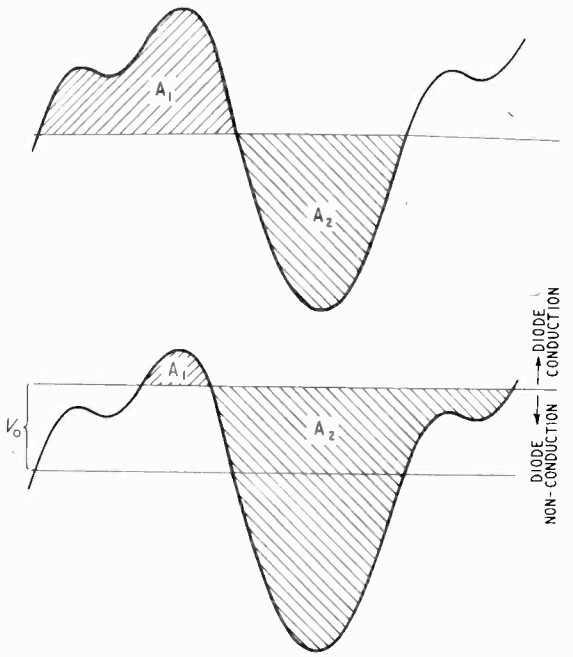

Fig. 3. *This diagram illustrates the input and grid-cathode voltages.*

positive areas multiplied by g_1 are equal to all negative areas multiplied by g_2 within one or more complete cycles. The level difference between the two dividing lines represents the amount of rectification V_0.

In the following paragraph the method is set out in detail. Fig. 4 illustrates the process.

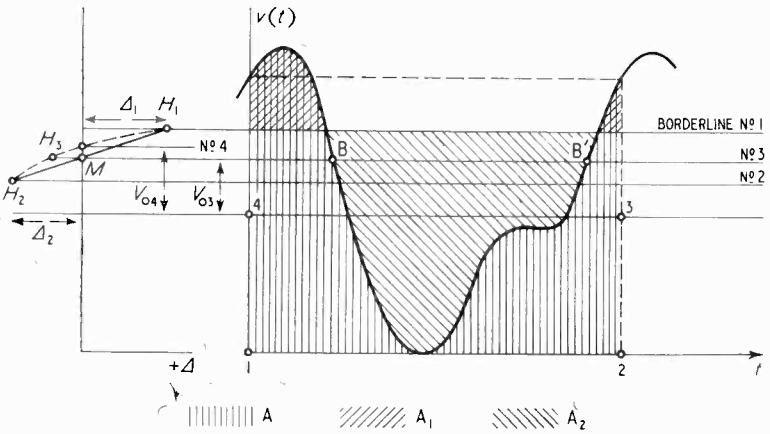

Fig. 4. *Graphical determination of the steady rectified voltage.*

1. Measure total areas A between the voltage curve and the time axis t, and the ordinates through points 1 and 2, spaced exactly one cycle apart. The measurement of area can be done either by a planimeter or by the counting of squares on graph paper.

2. Make rectangle 1 2 3 4 equivalent to area A. The level through 3 and 4 is the mean level of the voltage curve.

3. Calculate g_1 and g_2 from the circuit constants.

4. Draw tentative borderline No. 1.

5. Measure (or estimate) areas A_1 (i.e., all positive areas between curve and borderline No. 1) and A_2 (i.e., all negative areas between 1 and 2).

6. Calculate $\Delta_1 = g_1A_1 - g_2A_2$, a difference which should vanish for the correct position of the borderline.

7. Plot Δ_1, horizontally at the height of No. 1 borderline from an arbitrary reference line; mark point H_1. Draw another tentative borderline No. 2 with an attempt to reduce the difference Δ. Again measure areas above and below the new borderline No. 2, calculate the gA products, and the new difference Δ_2.

8. Plot Δ_2 horizontally at the height of No. 2 borderline to the right or left of the previous line, according to its sign, and mark point H_2.

9. Linearly interpolate (or extrapolate if the sign of Δ has not changed) the two results; i.e., draw a straight line through H_1 and H_2 and draw new borderline No. 3 through M.

10. No. 3 is a first approximation to the true border line so that V_{03} is a first approximation to the amount of rectification taking place. The points of intersection B and B' between borderline No. 3 and the curve mark the instants when the diode changes from conduction to non-conduction or vice versa.

11. If more accurate results are desired this process can be continued until the desired accuracy is achieved. The next step would then be to find Δ_3 for borderline No. 3, plot it as point H_3. Draw a tentative curve through H_1, H_2 and H_3. Where it cuts the reference line draw No. 4 borderline, etc.

Admittedly, this method is only tentative; one may have to carry out this graphical integration two or three times before the exact solution is approached to within a few per cent. The method is direct, however, and inherently applicable to any arbitrary wave shape which might not be mathematically expressible.

The distortion of wave shape occurring across the diode at P_3 of Fig. 1 (c) during the conducting phase can easily be determined by reducing the curve P_2 (Fig. 2) between t_0 and t_1 by the potential-divider ratio p_c (suffix c stands for conducting period) where

$$p_c = \frac{R_L r_D}{R_L + r_D} \Big/ \left(R_i + \frac{R_L r_D}{R_L + r_D} \right)$$

$$\approx \frac{r_D}{R_i + r_D} \quad \text{if } R_L \gg r_D \qquad \ldots \qquad (6)$$

whereas during the non-conducting phase the potential P_2 at any moment between t_1 and t_2 has only to be reduced by the factor

$$p_{nc} = \frac{R_L}{R_i + R_L} \qquad \ldots \qquad (6a)$$

Therefore the voltage wave across the diode is flattened out in the conducting phase to an extent which is the more pronounced the greater R_L and R_i compared with r_D. This property is often used for purposes of wave limitation, notably in pulse and television circuit technique. Hence it is particularly important to know what amount of limitation or flattening can be expected from a particular wave shape with a particular circuit arrangement, a question which can be

answered by this method. (See later remarks).

If a resistance R_s is connected in series with the diode, it is only necessary to substitute $(r_D + R_s)$ for r_D in the above formulae. During the conducting period the voltage across the diode itself will, of course, be a fraction $r_D/(r_D + R_s)$ of that across the combination.

The diode circuit most widely used for demodulating an a.m. wave is shown in Fig. 5. Here the capacitor discharges itself uninterruptedly through R_L; i.e., also during the phase of replenishing the lost charge. Hence the charging and discharging equations are

$$Q_1 = \int_{\phi_0}^{\phi_1} \frac{v - V_0}{R_i + r_D} d\phi = \frac{1}{R_i + r_D} \int_{\phi_0}^{\phi_1} (v - V_0) d\phi = g_1 A_1 \quad \ldots \quad (7)$$

and

$$Q_2 = \int_{\phi_0}^{\phi_2} \frac{V_0}{R_L} d\phi = \frac{V_0}{R_L}(\phi_2 - \phi_0) = g_2 A_2 \quad (8)$$

This case is particularly simple since equation (8) does not involve any real integration but merely the calculation of a rectangle of length $\phi_2 - \phi_0$ and height V_0 multiplied by $g_2 = \frac{1}{R_L}$.

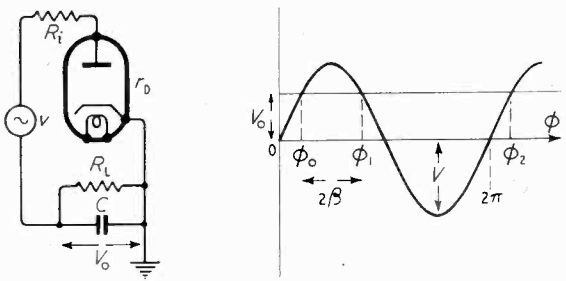

Fig. 5. *Typical a.m. detector circuit.*

Angles ϕ are used instead of time t because this case is analysed in detail in the appendix, and angles are a more convenient parameter if sine waves are used.

The cardinal stipulation of the present treatment is that the capacitor C which, during each cycle, receives a certain amount of charge, and loses it again during the rest of the cycle is assumed to be so large that the voltage increments across the capacitor are negligible compared with the quiescent voltage V_0.

3. Squaring Circuit

As a further example of the method Fig. 6 shows a double-diode circuit which is specially employed for distorting the wave shape; viz., for clipping a wave. If the problem arises of producing a nearly rectangular voltage from a sinusoidal one this double-diode clipper will perform the job by clipping a portion of the

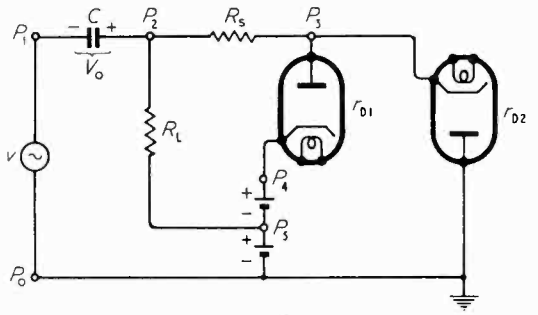

Fig. 6. *Double-diode clipping circuit.*

positive half sine wave, and a portion of the negative half sine wave, leaving a substantially trapezoidal wave. The source e.m.f. $P_1 = v(t)$ can be drawn (Fig. 7), and also P_2 on the assumption that the capacitor C will acquire a positive potential V_0. The battery potentials P_4 and P_5 will appear as parallel horizontal lines.

The capacitor C will accumulate negative charge on its right-hand plate from the instant t_0 onwards; viz., when P_2 rises above the steady potential P_5. The current flowing will be determined by the potential difference $P_2 - P_5$ and the resistance R_L. The accumulation of charge due to this branch of the circuit will continue until the instant t_3, when the current will change its direction and the negative charge will be withdrawn.

However, at the instant t_1 when $P_2 = P_4$ the first diode will start conducting, and C will accumulate charge through the path $R_s + r_{D1}$ as well as through the previous path. This new path will be open only until the instant t_2, hence the total negative charge accumulated is

$$Q_1 = Q_{1A} + Q_{1B} = \int_{t_0}^{t_3} \frac{P_2 - P_5}{R_L} dt + \int_{t_1}^{t_2} \frac{P_2 - P_4}{R_s + r_{D1}} dt \quad \ldots \quad (9)$$

Similarly the positive charge accumulated (or the negative charge withdrawn) consists of two parts; viz., the one through the leakage resistance R_L from t_3 to t_6, and the one through the other diode which conducts in the opposite direction, from t_4 to t_5. Hence

$$Q_2 = \int_{t_3}^{t_6} \frac{P_2 - P_5}{R_L} dt + \int_{t_4}^{t_5} \frac{P_2 - P_0}{R_s + r_{D2}} dt \quad (10)$$

The charging and discharging relations have

thus been established, and it merely remains to equate (9) and (10), and thus make their difference Δ vanish.

$$\Delta = \int_{t_0}^{t_3} \frac{P_2 - P_5}{R_L}\,dt + \int_{t_1}^{t_2} \frac{P_2 - P_4}{R_S + r_{D1}}\,dt - \int_{t_3}^{t_6} \frac{P_2 - P_5}{R_L}\,dt - \int_{t_4}^{t_5} \frac{P_2 - P_0}{R_S + r_{D2}}\,dt \quad (11)$$

or

$$\Delta = g_L A_{1A} + g_1 A_{1B} - g_L A_{2A} - g_2 A_{2B}$$

where

$$g_L = \frac{1}{R_L},\ g_1 = \frac{1}{R_S + r_{D1}},\ \text{and } g_2 = \frac{1}{R_S + r_{D2}}$$

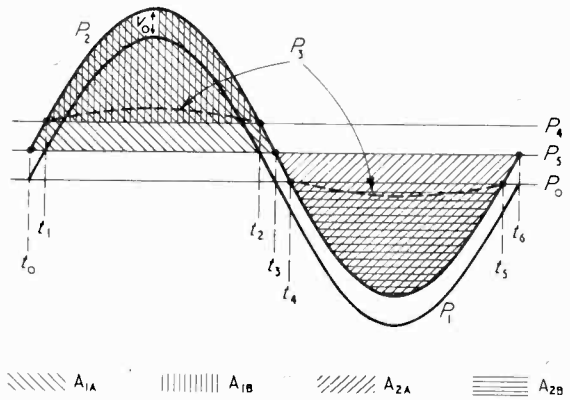

Fig. 7. *The action of the clipper of Fig. 6 is illustrated.*

The areas A_{1A}, A_{1B}, A_{2A} and A_{2B} are shaded in Fig. 7. In order to approach the final solution one must choose different positions of the parallel-line combination P_0 P_5 P_4 with respect to P_2, until the difference Δ vanishes. It is clear that in the case of any symmetrical wave with two identical diodes and $P_5 - P_0 = P_4 - P_5$ the solution will be very simple indeed and perfectly symmetrical.

The desired output curve of this clipping stage between P_3 and P_5 will be equal to $P_2 - P_5$ multiplied by the potential-divider ratio $r_D/(R_S + r_D)$. In order to make the clipped portions of P_3 as flat as possible diodes with a low resistance r_D must be used and R_S should be high. If R_S is too high, however, it will at higher frequencies cause a rounding off of the edges of the P_3 curve due to diode capacitance.

A few more practical examples may be of use in bringing the principles of this method of diode analysis into line with every-day engineering practice.

If for instance a diode circuit as depicted in Fig. 1 is to be used to flatten the top of the wave shown in Fig. 8, we first find the mean value of the curve, and indicate it by the line M. We then assume a certain amount of rectification V_0 and draw the line P_0. From the values of g_1 and g_2 and the fact that g_1 will always be greater than g_2, it follows that area A_1 must always be

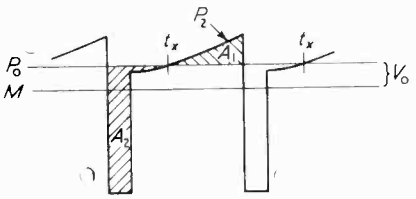

Fig. 8. *Flattening of the wave starts at t_x.*

smaller than area A_2 since $g_1 A_1 = g_2 A_2$; i.e., there will always be a positive V_0, which may, as shown in Fig. 8, prevent a complete cut of the undesirable top, for the flattening can only start at t_x. It is interesting to note that the rectification V_0 can be reduced by reducing the leakage resistance R_L to values below r_D. But this would reduce the signal very much, and the clipping effect would disappear.

A more successful approach would be the use of the circuit of Fig. 9. Here it is easier to make g_1 nearly equal to g_2 by making the series resistance R_S larger than the leak R_L, and yet without foregoing the clipping effect of the diode r_D. But again, there will always be a certain amount of rectification V_0. If rectification is to be cut out completely the capacitor C should be omitted, as well as the leak R_L. Then everything above zero (i.e., above the level M) will be clipped off.

If, however, the mean value M itself happens to cut the undesirable top as in Fig. 10 we must go one step further: we must employ rectification in the opposite sense, a process usually called d.c. restoration, and then apply the top clipping. This is shown in Fig. 11. The negative charge of the capacitor is neutralized through the restoration diode r_{D1}, so that $Q_2 = A_2/r_{D1}$. The assumed absence of a source impedance renders the areas A_2 very small, as little voltage drop across the low diode impedance r_{D1} is necessary to let comparatively heavy current pass through it. On the other hand the negative charge acquired passes through R_L (areas A'_1)

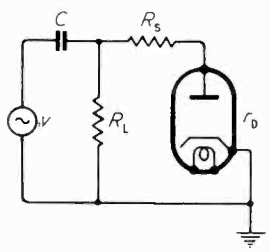

Fig. 9. *Circuit for flattening a wave but reducing the amount of rectification.*

and $R_S + r_{D2}$ (areas A_1) the latter only from potentials higher than the battery voltage P_4 onwards, so that $Q_1 = \frac{A'_1}{R_L} + \frac{A_1}{R_S + r_{D2}}$. It is not

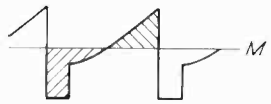

Fig. 10 *Wave with no rectification.*

intended to discuss here the merits and demerits of this particular application, it is introduced to illustrate this simple approach to diode circuits. If the peak value of a voltage wave is to be measured—as for instance in a valve voltmeter—the diode clipping effect should be reduced as far as possible, so that as small an area A_1 as possible will appear above zero level (see Fig. 2). From the previous analysis it follows that $R_i + \frac{R_L r_D}{R_L + r_D}$ should be as small as possible compared

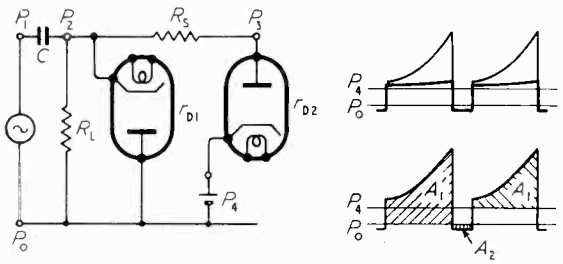

Fig. 11. *D.C. restoration with wave flattening.*

with $R_i + R_L$. As the diode resistance r_D and the source resistance R_i are given quantitites it appears that the only means of approach to real peak reading is to make R_L as high as possible. This is indeed quite customary in valve voltmeters where R_L is often made as high as 50 megohms.

4. Reactive Source Impedance

Considerations become a little more complicated however, if reactances are involved in the circuit. Two simple circuits may be mentioned. The first is the diode rectifying a voltage appearing across a tuned circuit as depicted in Fig. 12. The question arises again as to what amount of clipping will occur, because, after all, the internal impedance of the source is high; viz., $Z_i = Q\omega_0 L$. Closer contemplation will, however, reveal entirely different facts. The above formula for Z_i holds for a sinusoidal voltage at resonance frequency. The diode current represented by the areas A_1 is, however, anything but sinusoidal; in fact, it contains a total harmonic spectrum far in excess of the fundamental. For those harmonics the tuned circuit impedance is very low and almost purely capacitive. The diode pulse current will, therefore, produce little voltage drop across the source impedance. Hence, no noticeable clipping effect will occur. One can also reflect that the tuning capacitor acts as a reservoir ready to supply the short current pulses required by the diode without noticeable detriment to its total charge, hence its voltage will remain substantially unimpaired despite the presence of the diode.

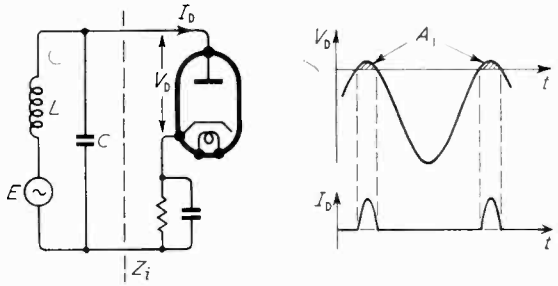

Fig. 12. *Conditions with a tuned circuit as a source impedance.*

Entirely different circumstances prevail if, for instance, the voltage induced in an inductance is to be measured with a diode rectifier. Suppose a coil is loosely coupled to a primary feeding coil as indicated in Fig. 13, then the equivalent circuit will show that the source impedance is high; viz., twice the leakage of the transformer. The previous arguments regarding the diode pulse current have to be entirely reversed as the harmonic content now finds a source impedance ever increasing with the order of the harmonics. Looking at it from the point of view of the

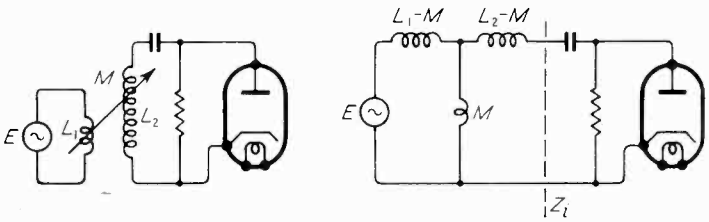

Fig. 13. *With an inductive source impedance the clipping action is accentuated.*

current pulses it is clear that the inductance will resist any sudden change of current through it by producing a corresponding back e.m.f. Consequently very heavy clipping can occur in such a case, and readings of a diode voltmeter will have to be carefully interpreted.

Finally it should be noted that the method described in this paper does not lend itself readily to reactive circuits such as have just been

mentioned, as it would involve graphical differentiation at every stage of the successive approximation. However, its implications do throw a significant light even on reactive circuits, and permit us to draw qualitative conclusions.

The analysis was developed for essentially non-reactive circuits, whereby it should be borne in mind that the capacitor C which we found to be vital for rectification, has virtually no reactance owing to its assumed infinite capacitance.

APPENDIX

A conventional diode circuit used for the demodulation of a.m. waves is to be analysed by the method outlined in the paper. Fig. 5 shows the circuit diagram, and the internal source impedance R_i is to be taken into account.

Capacitor C is charged to the constant value V_0. Charge Q_2 leaks away uninterruptedly through R_L, hence

$$Q_2 = \int_{\phi_0}^{\phi_2} \frac{V_0}{R_L}\, d\phi$$

It is replenished during the conducting period ϕ_0 to ϕ_1 by the amount

$$Q_1 = \int_{\phi_0}^{\phi_1} \frac{V_{max} \sin \phi - V_0}{R_i + r_D}\, d\phi$$

It is convenient to use angles ϕ instead of ωt.

From Fig. 5 we have

$\phi_1 - \phi_0 = 2\beta$, $\cos \beta = V_0/V_{max}$, $\phi_1 + \phi_0 = \pi$, and $\phi_2 - \phi_0 = 2\pi$

and since

$$\cos \alpha - \cos \beta = -2 \sin \frac{\alpha + \beta}{2} \sin \frac{\alpha - \beta}{2}$$

equating the two charges Q_1 and Q_2 gives

$$\frac{V_0}{R_L}[\phi_2 - \phi_0] = \frac{1}{R_i + r_D}[-V_{max}(\cos \phi_1 - \cos \phi_0) - V_0(\phi_1 - \phi_0)]$$

from which

$$\frac{V_0 2\pi}{R_L} = \frac{1}{R_i + r_D}[2 V_{max} \sin \beta - V_0 2\beta]$$

which may be written

$$\frac{R_i + r_D}{R_L}\pi = \tan \beta - \beta,$$

where

$$\cos \beta = \frac{V_0}{V_{max}}$$

This equation, also obtained in a different way by Everitt in his "Communication Engineering," page 429, cannot be solved mathematically by eliminating β, and expressing V_0 in terms of V and the circuit constants. It can only be solved graphically for β. Incidentally it also indicates that β is independent of signal amplitude and the arrangement is therefore a truly linear detector.

SYMMETRICAL MULTIVIBRATORS

Frequency and Waveform of Oscillation

By R. Feinberg, Dr.Ing., M.Sc.

(Electrical Engineering Dept., University of Manchester)

SUMMARY.—Formulae are derived from an equivalent circuit diagram to give the frequency and waveform of oscillation of a symmetrical multivibrator circuit with pentodes operating on the coalescent part of their characteristic; it is assumed that the interelectrode capacitances of the valves and any self-inductances and self-capacitances of the circuit elements have no effect on the circuit performance. The waveform of oscillation is rectangular when the time-constant of capacitor charge is relatively small, and is triangular when the time-constant is relatively large. The frequency is governed by the d.c. supply voltage, the type and screen-grid voltage of the pentodes and essentially by the values of the reservoir capacitance and the grid-shunting resistance. Predicted frequencies and waveforms are verified by experiment.

1. Introduction

THE importance of the multivibrator in circuit technique is generally recognized. Publications on the theory of multivibrator operation have so far been limited to the special case of rectangular waveform of oscillation.[1,2,3,4]

It was shown in another publication[5] that the multivibrator operation may be represented by a simple equivalent circuit diagram. It is the purpose of this paper to use the equivalent circuit diagram for the analysis of the performance of the symmetrical multivibrator with pentodes and to present formulae for the frequency and waveform of oscillation. It is assumed that the pentodes operate on the coalescent part of their characteristic and that the interelectrode valve capacitances and the self-capacitances and self-inductances of the circuit elements do not affect the performance.

MS accepted by the Editor, April, 1948.

2. Equivalent Multivibrator Diagram

Fig. 1 shows the multivibrator circuit and Fig. 2 gives the equivalent diagram in which the anode-paths of the pentodes V_A and V_B of Fig. 1 are replaced by a two-way switch S in series with

a resistor r_a, and the control-grid paths of V_A and V_B are represented by resistors r_{gA} and r_{gB} each in series with a unidirectional circuit element of zero voltage drop. The resistance of r_a corresponds to the gradient $\tan \phi = r_a$ of the coalescent part of the pentode characteristics, see Fig. 3.

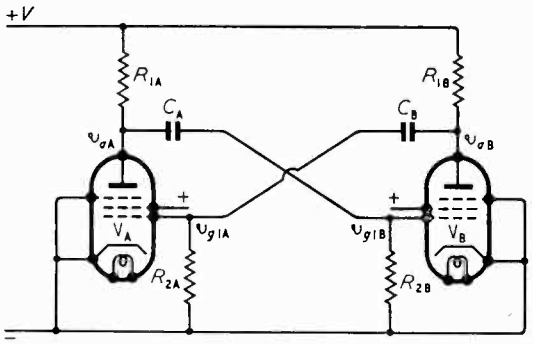

Fig. 1. *Multivibrator circuit.*

Switch S, of Fig. 2, in position A means that valve V_A of Fig. 1 is conducting and V_B is non-conducting, and vice versa when S is in position B. The reservoir capacitor C_A charges up when S is in position B and discharges when S is in position A; C_B charges up when S is in position A, and discharges when S is in position B. The discharging current from C_A produces across the resistor R_{2B} a voltage v_{g1B} of negative sign which controls the grid of the valve V_B and keeps V_B non-conducting until the discharging current from C_A has dropped to a critical value; at this critical value V_B becomes conductive initiating a trigger action between V_B and V_A as the consequence of which V_A becomes non-conductive.

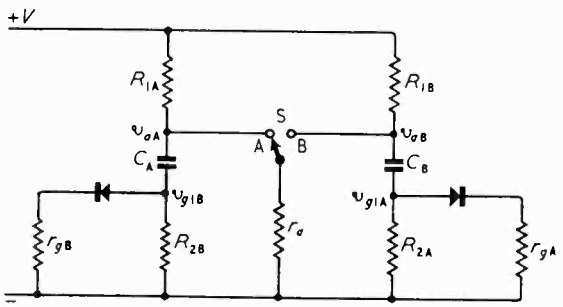

Fig. 2. *Equivalent multivibrator diagram.*

The trigger action means in terms of Fig. 2 that S commutates from A to B. C_B is now discharging, and the discharging current produces across R_{2A} a voltage v_{g1A} of negative sign which keeps V_A non-conductive until the discharging current from C_B has sufficiently dropped and commutation takes place from V_B to V_A. The cycle of action then starts again.

As the circuit is assumed to be symmetrical, the suffixes A and B can be omitted. Fig. 4 shows the circuit when C discharges. The circuit equations are, with the notation of Fig. 4,

$$v_g = -i_2R_2 = -v_c + i_3r_a \quad .. \quad .. \quad (1)$$

$$v_c = -\frac{1}{C}\int i_2 dt \quad .. \quad .. \quad .. \quad (2)$$

$$i_3r_a = V - i_1R_1 \quad .. \quad .. \quad .. \quad (3)$$

$$i_3 = i_1 + i_2 \quad .. \quad .. \quad .. \quad .. \quad (4)$$

The time-constant T_d of discharge is

$$T_d = C\left(R_2 + \frac{r_aR_1}{r_a + R_1}\right) \quad .. \quad .. \quad (5)$$

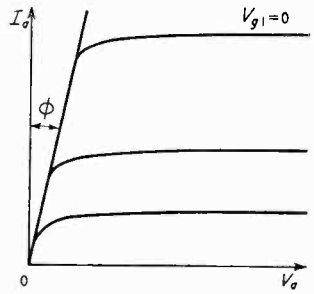

Fig. 3. *Pentode characteristics.*

The circuit for charging up C is shown in Fig. 5. The circuit equation is

$$V = \frac{T_c}{C}\cdot i + \frac{1}{C}\int i dt \quad .. \quad .. \quad .. \quad (6)$$

where

$$T_c = C\left(R_1 + \frac{r_gR_2}{r_g + R_2}\right) \quad .. \quad .. \quad (7)$$

is the time-constant of charging up.

3. Frequency of Oscillation

Fig. 6(a) gives a typical shape of the control-grid voltage v_g when the time-constant T_c of charging up C is relatively small, and Fig. 7(a) shows v_g when T_c is relatively large. The effect of T_c on v_g is apparent only in the positive half-periods when C charges up. In the negative half-periods C is discharging with the time-constant T_d.

In the negative half-periods v_g rises exponentially from an initial value V_g to the critical value v_{gc} at which the hitherto non-conductive valve becomes conductive and commutation takes place, see Figs. 6(a) and 7(a). Denoting by $T/2$ the half-period of oscillation, we have therefore with equation (5) the relation

$$\frac{v_{gc}}{V_g} = \exp\left(-\frac{T}{2T_d}\right) \quad .. \quad .. \quad .. \quad (8)$$

from which we obtain for the period T the equation

$$T = 2T_d \log_e \frac{V_g}{v_{gc}} \quad .. \quad .. \quad .. \quad (9)$$

The quantity v_{gc} in equation (9) is a constant fixed by the type of pentode used and the

magnitude of the screen-grid voltage. V_g is to be determined by solving equations (1) to (4).

For solving any of the differential equations arising from equations (1) to (4) a boundary condition is required. It is convenient to take as boundary condition the initial value V_c which the voltage v_c has at the beginning of the discharge of C. In the case corresponding to Fig. 6(a) C is practically charged to the d.c. supply voltage V, (see Fig. 5) before C begins to discharge; in this case we therefore have $V_c = V$ and equations (1) to (4) give

$$V_g = \frac{V}{1 + \frac{r_a}{R_1} + \frac{r_a}{R_2}} \quad .. \quad .. \quad .. \quad (10)$$

In the case corresponding to Fig. 7(a), C is charged to a value $V_c < V$ when the discharge begins. Therefore denote the initial value V_c of the capacitor voltage v_c by the expression

$$V_c = (1 - n)V \quad .. \quad .. \quad .. \quad .. \quad (11)$$

where $0 < n < 1$ is an unknown quantity. Equations (1) to (4) then give (see Appendix)

$$V_g = \frac{1 - n\left(1 + \frac{r_a}{R_1}\right)}{1 + \frac{r_a}{R_1} + \frac{r_a}{R_2}} V \quad .. \quad .. \quad (12)$$

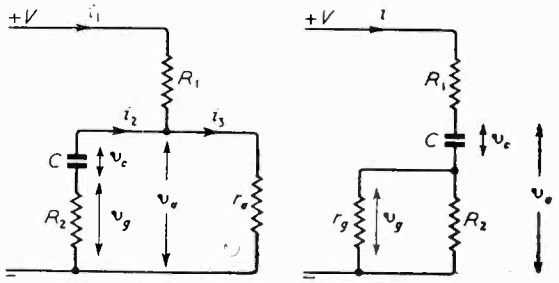

Fig. 4 (left). *Equivalent diagram for capacitor discharge.*

Fig. 5 (right). *Equivalent diagram for capacitor charge.*

To eliminate n from equation (12) follow up the change of v_c through a cycle of discharge and charge of C starting with V_c of equation (11) at the beginning of a discharge. At the end of the discharge period (i.e., after a time of length $T/2$) v_c has dropped to a value V_c' which is, according to Fig. 4 and equation (5), related to V_c by the expression

$$V_c' = V_c \exp\left(-\frac{T}{2T_d}\right) \quad .. \quad .. \quad (13)$$

In the subsequent charging period, also of length $T/2$, v_c rises from V_c' to V_c'' for which we have from Fig. 5 and equation (7) the relation

$$V_c'' = V - (V - V_c') \exp\left(-\frac{T}{2T_c}\right) \quad .. \quad (14)$$

As the multivibrator is considered to be in the steady state of operation we have the condition

$$V_c'' = V_c \quad .. \quad .. \quad .. \quad .. \quad (15)$$

Equations (11) and (13) to (15), therefore, give

$$n = \frac{\exp\left(\frac{T}{2T_d}\right) - 1}{\exp\left[\frac{T}{2T_d}\left(1 + \frac{T_d}{T_c}\right)\right] - 1} \quad .. \quad .. \quad (16)$$

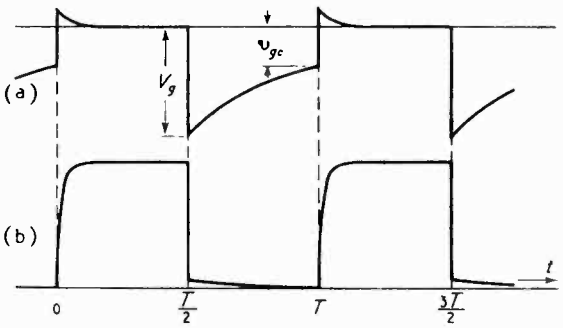

Fig. 6. *(a) Grid-control voltage v_g, and (b) anode voltage v_a for rectangular waveform of multivibrator oscillation.*

The unknown period T of multivibrator oscillation is found by solving equations (9), (12) and (16) for T. Substituting (16) in (12) and subsequently (12) in (9) leads to an unwieldy implicit equation for T. Therefore, another procedure for finding T is taken.

It is proposed to combine equations (9) and (12) to obtain an expression for $T/2T_d$ as a function of n, and to consider equation (16) as the second relation between $T/2T_d$ and n. The solution for $T/2T_d$, and hence T, is found by a graphical method.

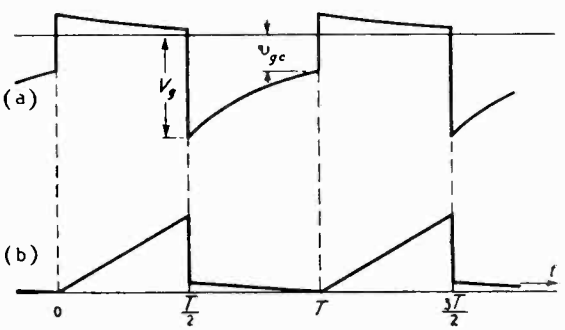

Fig. 7. *(a) Grid-control voltage v_g, and (b) anode voltage v_a for triangular waveform of multivibrator oscillation.*

The curves of Fig. 8 are drawn from equation (16) showing $T/2T_d$ against n with T_d/T_c as parameter. For $n = 0$ the curves become

coalescent and indefinite. From equations (9) and (12) we obtain

$$\frac{T}{2T_d} = \log_e \frac{V}{v_{gc}} - \log_e\left(1 + \frac{r_a}{R_1} + \frac{r_a}{R_2}\right) + \log_e\left[1 - n\left(1 + \frac{r_a}{R_1}\right)\right] \quad .. \quad (17)$$

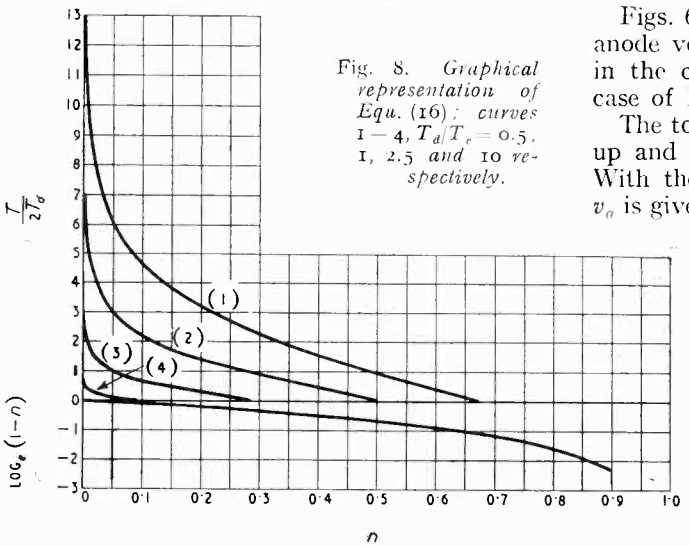

Fig. 8. *Graphical representation of Equ. (16); curves 1 — 4, T_d/T_c = 0.5, 1, 2.5 and 10 respectively.*

In a given problem $T/2T_d$ is found by drawing a $\frac{T}{2T_d} - n$ curve in the fashion of Fig. 8 and another $\frac{T}{2T_d} - n$ curve from equation (17). The intersection of both curves gives the solution for $T/2T_d$.

When $r_a \ll R_1$ and $r_a \ll R_2$, as is frequently the case, equation (17) is simplified to

$$\frac{T}{2T_d} = \log_e \frac{V}{v_{gc}} + \log_e (1 - n) \quad .. \quad .. \quad (18)$$

A curve showing $\log_e (1 - n)$ is drawn in the lower half of Fig. 8. It can be seen that the solution for $T/2T_d$ is little affected by n when $n < 0.1$. Therefore, when $n < 0.1$, equation (18) can be simplified to

$$\frac{T}{2T_d} = \log_e \frac{V}{v_{gc}} \quad .. \quad .. \quad .. \quad (19)$$

When $n < 0.1$ equation (19) gives immediately the solution for $T/2T_d$.

Equations (17) and (16) show that the frequency of multivibrator oscillation is governed by the d.c. supply voltage V, the critical grid-voltage v_{gc}, which is fixed by the type of pentode used and the screen-grid voltage applied, and by the time-constant T_d of capacitor discharge. The time-constant T_c of capacitor charge has in general only a small influence on the frequency of oscillation. The influence of T_c is practically nil when the ratio of T_c to T_d is relatively small; note, e.g., in Fig. 8, that $T_d/T_c > 10$ when $n < 0.1$. Practically speaking $n = 0$ in equation (18).

4. Waveform of Oscillation

Figs. 6(b) and 7(b) show typical shapes of the anode voltage v_a. The waveform is rectangular in the case of Fig. 6(b) and triangular in the case of Fig. 7(b).

The top-section of v_a is formed when C charges up and the bottom section when C discharges. With the notation of Fig. 5 the top section of v_a is given by the relation

$$v_a = V - iR_1 \quad .. \quad .. \quad (20)$$

Solving (6) for i with (13) and (11) we get from (20)

$$\frac{v_a}{V} = 1 - \frac{CR_1}{T_c}\left[1 - (1 - n)\exp\left(-\frac{T}{2T_d}\right)\right] \times \exp\left(-\frac{2t}{T}\cdot\frac{T}{2T_c}\right) \quad .. \quad (21)$$

The value of n to be inserted is found when solving (9), (12) and (16) for $T/2T_d$.

For the bottom section of v_a we have with the notation of Fig. 4 the equation

$$v_a = i_3 r_a \quad .. \quad .. \quad .. \quad .. \quad .. \quad (22)$$

Solving equations (1) to (4) for i_3 we obtain, with (12) and (9) and with the time-notation of Fig. 7(b), (see Appendix), the expression

$$\frac{v_a}{V} = \frac{r_a}{r_a + R_1}\left\{1 + \frac{R_1}{R_2}\frac{v_{gc}}{V}\exp\left[\frac{T}{2T_d}\left(2 - \frac{2t}{T}\right)\right]\right\} \quad .. \quad .. \quad .. \quad (23)$$

When $r_a \ll R_1$ and $r_a \ll R_2$ equation (23) for the bottom section of v_a becomes approximately

$$v_a/V = 0 \quad .. \quad .. \quad .. \quad .. \quad .. \quad (24)$$

and equation (21) for the top section of v_a becomes, with (8) and with $V_g = (1 - n)V$ derived from (12)

$$\frac{v_a}{V} = 1 - \frac{CR_1}{T_c}\left(1 - \frac{v_{gc}}{V}\right)\exp\left(-\frac{2t}{T}\frac{T}{2T_c}\right) \quad (25)$$

If $r_g \ll R_1$ and $r_g \ll R_2$ (7) shows that $T_c = CR_1$. If also $v_{gc} \ll V$ then (25) is simplified to

$$\frac{v_a}{V} = 1 - \exp\left(-\frac{2t}{T}\frac{T}{2T_c}\right) \quad .. \quad .. \quad (26)$$

Fig. 9 shows various waveforms of v_a/V calculated from equations (26) and (24) with $T/2T_c$ as parameter. The waveform is triangular for $T/2T_c < 2$ and rectangular when $T/2T_c > 10$.

The ratio $T/2T_c$ is conveniently designated

the waveform co-efficient of the multivibrator circuit. Since $\frac{T}{2T_c} = \frac{T}{2T_d} \cdot \frac{T_d}{T_c}$, and $T/2T_d$ is almost independent of T_d/T_c according to Fig. 8 and equation (17) it can be seen that the waveform remains practically unaltered if the frequency of oscillation is changed in a given circuit by varying the value of C. On the other hand, the frequency of oscillation is almost unaffected if in a given circuit the waveform is changed by altering the value of the anode resistance R_1.

5. Examples

Valve data: Type VR56 = EF6.

$v_{gc} = 4.9$ volts (95 volts at the screen-grid).

$r_a = 2200\ \Omega$.

$r_g = 1100\ \Omega$.

D.C. supply: $V = 100$ volts.

(1) $R_1 = 50.2$ kΩ, $R_2 = 685$ kΩ.

Since $r_a \ll R_1$ and $r_a \ll R_2$ apply equation (18) and obtain with the given data for V and v_{gc}:—

$$T/2T_d = 3 + \log_e (1 - n) \quad .. \quad .. \quad \text{(i)}$$

From equation (5)

$$T_d = CR_2 \quad .. \quad .. \quad .. \quad .. \quad \text{(ii)}$$

Since $r_g \ll R_1$ and $r_g \ll R_2$ equation (7) gives

$$T_c = CR_1 \quad .. \quad .. \quad .. \quad .. \quad \text{(iii)}$$

Therefore, with equation (ii)

$$T_d/T_c = R_2/R_1. \quad .. \quad .. \quad .. \quad \text{(iv)}$$

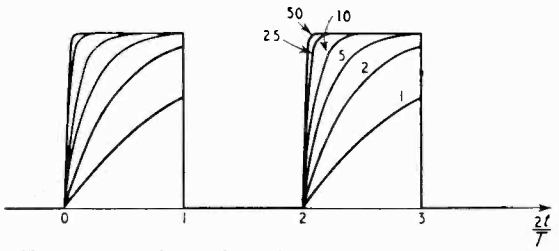

Fig. 9. *Waveform of multivibrator oscillation; values of $T/2T_c$ are marked on the curves.*

With the given data for R_1 and R_2 we get $T_d/T_c = 13.7$. Equation (i) and Fig. 8 show that the solution for $T/2T_d$ with $T_d/T_c = 13.7$ is at $n = 0$. Therefore, from (i) and (ii), we obtain for the predicted frequency $f_p = 1/T$ the expression

$$f_p = 1/6CR_2 \quad .. \quad .. \quad .. \quad .. \quad \text{(v)}$$

Let f_m denote the frequency observed by experiment. The following results were found:—

Case (a): $C = 0.00021\ \mu$F; $f_p = 1150$ c/s, $f_m = 1050$ c/s.

Case (b): $C = 0.002\ \mu$F; $f_p = 122$ c/s, $f_m = 120$ c/s.

Prediction and experimental result are in fair agreement, the discrepancy being about 8% and 2% respectively.

The waveform coefficient is $\frac{T}{2T_c} = \frac{T}{2T_d} \cdot \frac{T_d}{T_c}$ $= 3 \times 13.7 = 41.1$. Consequently v_a/V should be similar to curve (6) in Fig. 9 and independent of C. The prediction is verified by the oscillograms (a) and (b) in Fig. 10.

(2) $R_1 = 50.2$ kΩ, $R_2 = 70.2$ kΩ.

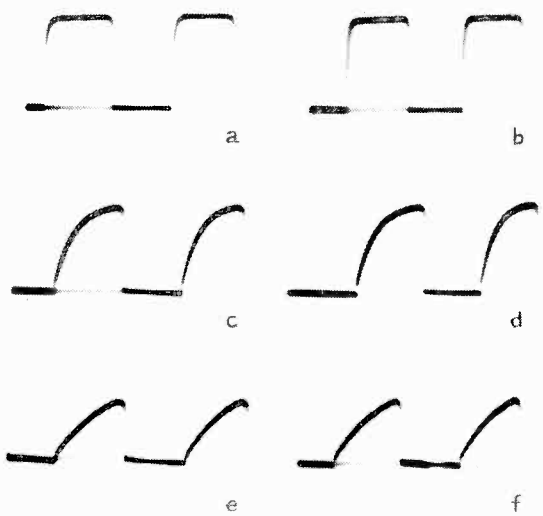

Fig. 10. *Oscillograms of multivibrator oscillations:—*
a: $R_1 = 50.2$ kΩ, $R_2 = 685$ kΩ, $C = 0.00021$ μF, $f_m = 1060$ c/s.
b: $R_1 = 50.2$ kΩ, $R_2 = 685$ kΩ, $C = 0.002$ μF, $f_m = 120$ c/s.
c: $R_1 = 50.2$ kΩ, $R_2 = 70.2$ kΩ, $C = 0.001$ μF, $f_m = 2240$ c/s.
d: $R_1 = 50.2$ kΩ, $R_2 = 70.2$ kΩ, $C = 0.01$ μF, $f_m = 232$ c/s.
e: $R_1 = 50.2$ kΩ, $R_2 = 25$ kΩ, $C = 0.001$ μF, $f_m = 6250$ c/s.
f: $R_1 = 50.2$ kΩ, $R_2 = 25$ kΩ, $C = 0.01$ μF, $f_m = 630$ c/s.

Equation (iv) gives $T_d/T_c = 1.4$. First estimate the probable value of n to avoid any unnecessary plotting of a $\frac{T}{2T_d} - n$ curve from (16). Equation (i) and Fig. 8 show that $n < 0.05$ which means that practically $n = 0$. Therefore, (v) is applicable. With the given value of R_2:—

Case (c): $C = 0.001\ \mu$F; $f_p = 2380$ c/s, $f_m = 2240$ c/s.

Case (d): $C = 0.01\ \mu$F; $f_p = 238$ c/s, $f_m = 232$ c/s.

Prediction and measurement agree fairly closely, the discrepancy being about 6% and 2.5% respectively.

The waveform coefficient is $T/2T_c = 3 \times 1.4 = 4.2$. v_a/V should be similar to curve (3) in Fig. 9 and independent of C. This is verified by the oscillograms (c) and (d) in Fig. 10.

(3) $R_1 = 50.2$ kΩ, $R_2 = 25$ kΩ.

Equation (iv) gives $T_d/T_c = 0.5$. From equation

(i) and Fig. 8 with $T_d/T_c = 0.5$ we obtain $T/2T_d = 2.8$. The predicted frequency therefore becomes with (ii)

$$f_p = 1/5.6CR_2 \quad .. \quad .. \quad .. \quad .. \quad \text{(vi)}$$

The observations were :—

Case (e) : $C = 0.001\ \mu F$; $f_p = 7150$ c/s, $f_m = 6250$ c/s.

Case (f) : $C = 0.01\ \mu F$; $f_p = 715$ c/s, $f_m = 630$ c/s.

Prediction and measurement are in reasonable agreement, the discrepancy being about 12%.

The waveform coefficient is $T/2T_c = 2.8 \times 0.5 = 1.4$. The shape of v_a/V should therefore be between the curves for values of 1 and 2 in Fig. 9. This is verified by the oscillograms (e) and (f) of Fig. 10.

REFERENCES

1 H. Abraham and E. Bloch, "Mesure en valeur absolue des périodes des oscillations électriques de haute fréquence." *Annal. Physique*, 1919, Vol. 12, p. 237.

2 F. C. Williams and A. Fairweather, "A 'Chopped-Signal' Vacuum Tube Generator with Good Voltage Regulation," *P.O. elect. Engrs' J.*, 1939, Vol. 32, p. 104.

3 F. Vecchiacchi, "Meccanismo di funzionamento e frequenza del multivibratore." *Alta Frequenza*, 1940, Vol. 9, p. 745.

4 M. V. Kiebert, Jr., and A. F. Inglis, "Multivibrator Circuits," *Proc. Inst. Radio Engrs*, 1945, Vol. 33, p. 534. See also *Wireless Engineer*, Dec., 1945, p. 573.

5 R. Feinberg, "On the Performance of the Push-Pull Relaxation Oscillator (Multivibrator)," *Phil. Mag.*, 1948, Series 7, Vol. 29, p. 268.

APPENDIX

Elimination of i_1 and i_3 from equations (1) to (4) leads to the differential equation

$$\frac{di_2}{dt} = -\frac{i_2}{T_d} \quad .. \quad .. \quad .. \quad .. \quad .. \quad \text{(a)}$$

with T_d defined by equation (5). We therefore obtain

$$i_2 = A \exp\left(-\frac{t}{T_d}\right) \quad .. \quad .. \quad .. \quad .. \quad \text{(b)}$$

and subsequently

$$i_1 = \frac{V}{r_a + R_1} - \frac{r_a}{r_a + R_1} A \exp\left(-\frac{t}{T_d}\right) \quad \text{(c)}$$

$$i_3 = \frac{V}{r_a + R_1} + \frac{R_1}{r_1 + R_1} A \exp\left(-\frac{t}{T_d}\right) \quad \text{(d)}$$

with A as the integration constant.

In order to determine A write from (1)

$$v_c = i_2 R_2 + i_3 r_a \quad .. \quad .. \quad .. \quad .. \quad \text{(e)}$$

and with equation (b), (d) and (5)

$$v_c = V \frac{r_a}{r_a + R_1} + \frac{T_d}{C} A \exp\left(-\frac{t}{T_d}\right) \quad .. \quad \text{(f)}$$

When $t = 0$; $v_{c(t=0)} = V_c$, and from equation (f) with the notation of (11)

$$A = V \frac{C}{T_d}\left(\frac{R_1}{r_a + R_1} - n\right) \quad .. \quad .. \quad .. \quad \text{(g)}$$

V_g of equation (12) can be found by writing from equation (1)

$$v_g = -i_2 R_2 \quad .. \quad .. \quad .. \quad .. \quad .. \quad \text{(h)}$$

At $t = 0$ we have $-v_{g(t=0)} = V_g$. Equations (b) and (g) substituted in (h) give for V_g the expression

$$V_g = \frac{CR_2}{T_d}\left(\frac{R_1}{r_a + R_1} - n\right) V \quad .. \quad .. \quad \text{(i)}$$

which with (5) leads to (12)

Substituting (i) in (g) we derive from equations (c), (b) and (d)

$$i_1 = \frac{V}{r_a + R_1}\left[1 - \frac{r_a}{R_2}\frac{V_g}{V} \exp\left(-\frac{t}{T_d}\right)\right] \quad .. \quad \text{(j)}$$

$$i_2 = \frac{V_g}{R_2}\exp\left(-\frac{t}{T_d}\right) \quad .. \quad .. \quad .. \quad .. \quad \text{(k)}$$

$$i_3 = \frac{V}{r_a + R_1}\left[1 + \frac{R_1}{R_2}\frac{V_g}{V} \exp\left(-\frac{t}{T_d}\right)\right] \quad \text{(l)}$$

Equation (1) with the time-notation of Fig. 7(b) and with (8) and (22) give equation (23).

NEW BOOKS

Laufzeittheorie der Elektronenröhren, Vols. I and II.

By DR. H. W. KÖNIG. Pp. 354 + xii with 119 Figs. Springer-Verlag, Mölkerbastei, 5, Wien I, Austria. Price £3 14s. 6d. (Vols. I and II).

This work is in two volumes, but the numbering of the pages and figures is continuous. It deals with the transit-time theory as applied to valves and tubes. It is necessarily very mathematical. The first volume is entitled Ein-und Mehrkreissysteme and the second, Kathodeneigenschaften, Vierpole. In the preface it is stated that it is a collection of articles written with the object of publication in technical journals, but the war made this impossible, and in view of the length and number of the articles it was decided to publish them as a book. The first volume contains four sections dealing with increasing numbers of electrodes, but all based on the assumption that the electrons leave the cathode with zero velocity. The second volume, in which this assumption is not made, contains six sections dealing with space charge, cathode properties, shot effect, noise, Barkhausen-Kurz effect, klystrons, etc. The last forty pages are devoted to the application of four-pole theory to valves. The wording is unusual but one soon gets used to regarding a tetrode as a Zweikreis-Dreikammersystem. In the early days of valves the frequencies were such that the passage of the electron through the valve occupied a negligible fraction of the period, but with the advent of dm and cm waves this was no longer the case, and the electron could no longer be assumed to pass from cathode to anode in a quasi-static electric field ; the transit time became an appreciable fraction of the period, with resulting complexities in the theory. One can almost say that this book begins where most books on valves finish, since transit time is taken into account from the very beginning. The treatment is very thorough and very clear. The book is well produced, the printing is excellent and there is no suggestion of austerity. Every section concludes with a bibliography. It can be unreservedly recommended to anyone with a knowledge of German who wishes to gain a clear conception of the internal operation of valves, klystrons, travelling-wave tubes, etc. G. W. O. H.

Resonant Absorbers and Reverberation.

Pp. 57. The Physical Society, 1, Lowther Gardens, Prince Consort Rd., London, S.W.7. Price 7s. 6d.

This publication contains papers and discussions of the first summer symposium (1947) of the Acoustics Group on Sound Absorption and Reverberation.

Introductory Radio (Theory and Servicing)

By H. J. HICKS. Pp. 393 + vii. McGraw-Hill Publishing Co., Ltd., Aldwych House, London, W.C.2. Price 19s. 6d. (In U.K.).

OSCILLATION AMPLITUDE IN SIMPLE VALVE OSCILLATORS

By A. S. Gladwin, B.Sc., A.M.I.E.E.

(*King's College, University of London*)

SUMMARY. A method is derived of calculating the oscillation amplitude in simple valve oscillators of the regenerative type where grid-leak bias is used. The amplitude is found in terms of parameters which are functions of the valve and circuit constants, and the solution is presented in graphical form.

Two types of amplitude instability are studied and criteria for their existence are deduced. The first type is dynamical instability or squegging; the second type gives rise to the effect known as oscillation hysteresis.

The analysis is applicable to all the common types of oscillator circuits subject to the conditions that the valve should operate always in the space-charge-limited condition, and that the anode voltage should never fall to the point where the anode current is rapidly diverted to the grid or screen.

1. Introduction

THE oscillators to be considered are of the regenerative type shown diagrammatically in Fig. 1, in which the electrodes of a thermionic valve are coupled together by a frequency-selective network, the chief part of which is an oscillatory circuit OC. For convenience the valve is shown as a triode, but the analysis is equally applicable to tetrode and pentode valves. The oscillation amplitude is limited by applying to the grid a negative biasing voltage produced by the flow of grid current through a high resistance R_g.

The main object of the investigation is to calculate the steady-state value of the oscillation amplitude; i.e., the alternating grid voltage. Existing methods[1] of calculating the performance of such oscillators begin by assuming certain operating conditions for the valve, including the amplitudes of the grid and anode alternating voltages and the grid-bias voltage, and deducing therefrom the constants of the feedback network required to satisfy the assumed conditions. These conditions are usually such as to produce the maximum power output from the oscillator.

In many circumstances, however, the problem to be solved is the converse of this. The constants of the feedback network are fixed by considerations other than those of optimum operating conditions for the valve, and it is required to find the amplitude of oscillation which corresponds to the given network constants. An example of such a problem is the oscillator in a superheterodyne receiver. Efficiency is not usually of first importance in these oscillators and may be small, as in the example quoted.

The problem could be solved, using existing methods, by calculating for several assumed values of oscillation amplitude the corresponding values of some constant of the feedback network (e.g., the dynamic resistance of the oscillatory circuit, assuming this to be the variable), and constructing a graph from which the amplitude corresponding to any other value of the dynamic resistance could be read off. If more than one constant of the network were varied many sets of graphs would be required to cover all the possible combinations.

When an accurate solution is called for this is probably the only satisfactory method, but it is clearly very tedious, particularly when, as is usual, many constants of the feedback network must be taken into account. In most problems of this kind, however, an approximate solution is all that is required. Precise calculations are seldom justified, as the primary data are not usually known with any great accuracy. An approximate general solution has been obtained in the form of a set of graphs which are applicable to all the simple types of circuits. The results are sufficiently accurate for all practical purposes.

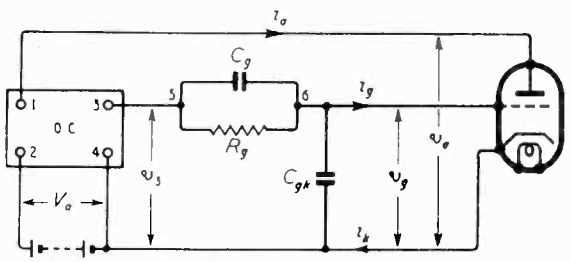

Fig. 1. *Oscillator circuit.*

The method of analysis is to examine separately the feedback network, the grid current and grid voltage, and the anode current. Finally, the various quantities are grouped together to form a few parameters which are plotted as a family

MS accepted by the Editor, December 1947; revised April 1948.

of curves. From these the oscillation amplitude can easily be found by the method explained in Section 6.

The calculated value of oscillation amplitude is attained only if this amplitude corresponds to a stable state of oscillation. Amplitude instability may take the form of a periodic modulation or interruption of the amplitude—an effect commonly known as squegging. As is well known, this can always be stopped by reducing the value of the grid capacitor C_g.

Another kind of instability is manifest in the effect known as oscillation hysteresis. As the coupling between anode and grid is varied, points are found where the oscillation amplitude jumps from one stable value to another, the critical points and the critical amplitudes being different according to the direction from which they are approached. The various forms of instability are studied in some detail and criteria for their existence are deduced.

Certain assumptions are made in order to simplify the analysis. Perhaps the most important of these is that the valve operates always in such a way that the space current and the electrode potentials are connected by the well-known three-halves power law. The effect of this assumption is to restrict the analysis to oscillators in which the alternating anode voltage is not a large fraction of the h.t. supply voltage, and thus to exclude oscillators of high efficiency. Various other assumptions are made concerning the valve and feedback network. These are explained at the appropriate points in the text. Experiment shows that these assumptions do not lead to serious error.

2. Principal Symbols

b_a, b_g = Constants of the valve (see text Section 6).
C_g = Capacitance of the grid-bias capacitor.
c_{gk} = Grid-cathode capacitance of the valve.
G_t = Transfer conductance of the feedback network at the oscillation frequency.
i_a = Anode current.
i_{a1} = Anode current of oscillation frequency.
i_g = Grid current.
i_{g1} = Grid current of oscillation frequency.
I_{g1} = Amplitude of grid current of oscillation frequency.
I_g = Mean grid current.
K, N = Functions of the valve and circuit constants. (See equations 5.3 and 5.4.)
ϕ = Conduction half-angle for the grid current.
Q = Ratio of reactance to effective series resistance in the feedback network.
R_g = Grid bias resistance.
r_g = Grid input resistance at the oscillation frequency.
R_t = Input resistance of the feedback network at the oscillation frequency.
μ = Amplification factor of the valve.
v_a = Anode voltage.
v_{a1} = Anode voltage of the oscillation frequency.
V_{a1} = Amplitude of the anode voltage of oscillation frequency in antiphase with v_g.
v_g = Grid voltage.
V_g = Mean grid voltage.
v_{g1} = Grid voltage of the oscillation frequency.
V_{g1} = Amplitude of the grid voltage of oscillation frequency.
V_{ca} = Grid voltage at anode current cut-off point.
V_{cg} = Grid voltage at grid current cut-off point.
ω_0 = Oscillation angular frequency, radians/sec.
ω_s = Modulation angular frequency, radians/sec.
X_g = $1/\omega_0 (C_g + c_{gk})$.
$Y_t(j\omega)$ = Transfer admittance of the feedback network.
$Z_i(j\omega)$ = Input impedance of the feedback network.

3. The Feedback Network

The feedback network comprises the circuit elements lying between terminals 1, 2 and 6, 4 in Fig. 1 of which the most important is an oscillatory circuit denoted by OC. This may be of the Hartley or Colpitts type or any other of the simple and well-known arrangements. An appropriate decoupling circuit for the h.t. supply is supposed to be included.

The object of this Section is to formulate some relations between the currents and voltages in the network for use in later parts of the paper.

It is convenient to consider the interelectrode capacitances of the valve as belonging to the feedback network. Of these the most important is usually the grid-cathode capacitance c_{gk}. If a multi-grid valve were used instead of a triode c_{gk} would be replaced by the capacitance between the grid and the electrodes which are at cathode potential with respect to high-frequency voltages. The anode-cathode and grid-anode capacitances are not shown in Fig. 1. The former is equivalent to a capacitor connected between 1 and 2. In inductively coupled networks the grid-anode capacitance has a negligible effect on the oscillation amplitude, but in circuits such as the tuned-grid tuned-anode type one or other of these capacitances plays a major part in producing regeneration and must therefore be included in the calculation of the network constants. The significance of c_{gk} for the analysis is that it forms together with C_g a high-frequency potentiometer which may produce appreciable attenuation between terminals 5 and 6.

It is also convenient to consider the grid input resistance r_g of the valve, at the oscillation frequency, as if it were a physical resistor connected between 6 and 4 and formed part of the feedback network.

For the purpose of the analysis the most important parameters of the network are the transfer admittance $Y_t\ (j\omega)$ between 1, 2 and 6, 4, the input impedance $Z_i\ (j\omega)$ between 1 and 2, the output impedance $Z_0\ (j\omega)$ between 6 and 4 with the valve inoperative, and the Q factor.

Elementary circuit analysis shows that, at frequencies close to the resonant frequency ω_r of the oscillatory circuit, the transfer admittance between 1, 2 and 6, 4 (i.e., the ratio of the current flowing from 1 to 2 to the voltage between 6 and 4 produced by this current), can be expressed for all kinds of networks, in the form

$$Y_t\ (j\omega) = G_t\{1 + j2Q\ (\omega/\omega_r - 1)\}$$

where $Q = \omega_r\ L/R$, and L is the inductance and R the equivalent series resistance of the oscillatory circuit.

It is assumed that the oscillation frequency ω_0 is equal to ω_r. In fact, for various reasons, this is never quite true, but the reactive component of $Y_t\ (j\omega)$ is always very small at the oscillation frequency, and has a negligible effect on the oscillation amplitude. It is therefore permissible to write

$$Y_t\ (j\omega) = G_t\{1 + j2Q\ (\omega/\omega_0 - 1)\} \quad . . \quad (3.1)$$

G_t is the transfer conductance at the oscillation frequency, and in order that the grid voltage should be of the correct phase to maintain oscillation, G_t must be negative.

The current flowing into the network at 1 is equal and opposite to the anode current of the valve. (The currents and voltages shown in Fig. 1 are conventionally positive and the cathode potential is taken as zero.) Hence, if i_{a1} and v_{g1} are the anode current and grid voltage of fundamental frequency

$$v_{g1} = -\ i_{a1}/G_t$$

$$\text{and } V_{g1} = -\ I_{a1}/G_t \quad . . \quad . . \quad . . \quad (3.2)$$

At harmonic frequencies a difficulty arises because the harmonic grid currents depend mainly on the fundamental grid voltage and little on the harmonic grid voltages. The concept of grid input impedance is therefore not a very useful one at harmonic frequencies. However, it is not usually required to calculate the harmonic amplitudes with great accuracy, so for this purpose the harmonic grid currents can be neglected; i.e., the grid input impedance at harmonic frequencies is assumed to be infinite.

If the anode current of n^{th} harmonic frequency is i_{an} the corresponding harmonic grid voltage is

$$v_{gn} = -\ i_{an}/Y_t\ (jn\omega_0)$$

$$= -\ i_{an}/(G_{tn} + jB_{tn})$$

In practice the precise value of G_{tn} may be difficult to determine, because of the variation of resistance with frequency, but in all the simple networks it is small compared with B_{tn} and G_t, and may be neglected. Then

$$v_{gn} = j\ i_{an}/B_{tn}$$

It is shown in Section 5 that the fundamental and harmonic anode currents reach their maxima almost simultaneously. The anode current may be written approximately as

$$I_a + \sum_{1}^{\infty} I_{an} \cos n\omega_0 t \quad . . \quad . . \quad (3.3)$$

and the alternating grid voltage is therefore

$$v_{ga} = V_{g1} \cos \omega_0 t + \sum_{2}^{\infty} V_{gn} \sin n\omega_0 t \quad (3.4)$$

where $V_{gn} = -\ I_{an}/B_{tn}$

$$\text{and } \frac{V_{gn}}{V_{g1}} = \frac{I_{an}}{I_{a1}} \cdot \frac{G_t}{B_{tn}} \quad . . \quad . . \quad . . \quad (3.5)$$

The ratio G_t/B_{tn} is inversely proportional to Q. It is assumed that Q is always large, so that the harmonic voltages are only a few per cent of the fundamental.

So far as the input impedance $Z_i(j\omega)$ between 1 and 2 is concerned, feedback networks may be divided into two classes. In networks of the first class, which includes the Hartley and Colpitts types, $Z_i(j\omega)$ is comparable with $-1/G_t$ at the oscillation frequency and is equal to a resistance R_i at that frequency. In networks of the second class, which are exemplified by a parallel-resonant circuit connected between 3 and 4 with a coupling coil between 1 and 2, $Z_i(j\omega)$ is usually small compared with $-1/G_t$ and, depending on the coefficient of coupling between the coils, has a reactive component which may be large or small compared with the resistive component. For both classes of network it is easily shown that at frequencies near the oscillation frequency

$$Z_i = jX_i + R_i/\{1 + j2Q(\omega/\omega_0 - 1)\} \quad . . \quad (3.6)$$

X_i is zero in networks of the first class.

The anode current of oscillation frequency is

$$i_{a1} = I_{a1} \cos \omega_0 t$$

Then the anode voltage of oscillation frequency is

$$-\ (R_i + jX_i)\ i_{a1}$$

$$= -\ V_{a1} \cos \omega_0 t + \frac{V_{a1} X_i}{R_i} \sin \omega_0 t$$

where $V_{a1} = R_i\ I_{a1} = -\ G_t R_i\ V_{g1} \quad . . \quad (3.7)$

At harmonic frequencies $Z_i(j\omega)$ is almost wholly reactive.

$$Z_i(jn\omega_0) = jX_{in}$$

Assuming the anode current to be given by (3.3) the alternating anode voltage is

$$v_{aa} = -\ V_{a1} \cos \omega_{0t} + \frac{V_{a1} X_i}{R_i} \sin\ \omega_0 t + \sum_{2}^{\infty} V_{an} \sin n\omega_0 t \quad . . \quad . . \quad . . \quad (3.8)$$

where $V_{an} = I_{an}\ X_{in}$

In connection with the study of amplitude instability it is necessary to know what effect changes in the grid input resistance have on the values of G_t and R_i.

Suppose that the power supplies to the valve are disconnected so that the grid input resistance becomes infinite. Let the impedance between terminals 6 and 4 at the oscillation frequency then be $R_0 + jX_0$. Now let a current of frequency ω_0 flow into 1, and let the voltage at 6 be v. If a resistor of value r_g is then connected between 6 and 4 the voltage at 6 becomes, by Thévenin's theorem

$$\frac{vr_g}{r_g + R_0 + jX_0}$$

By definition, the transfer conductance is

$$G_t = \frac{i}{v} \cdot \frac{r_g + R_0 + jX_0}{r_g}$$

If r_g is altered to r'_g the transfer admittance becomes

$$Y_t'(j\omega.) = \frac{i}{v} \cdot \frac{r'_g + R_0 + jX_0}{r'_g}$$

It is clear that $Y'_t\ (j\omega_0)$ now has a reactive component so that the frequency at which $Y'_t(j\omega)$ is wholly real is different from ω_0. It may be assumed that for all practical values of r'_g this difference is very small, and also that X_0 is small compared with $R_0 + r'_g$. Hence if G'_t is the transfer conductance corresponding to r'_g

$$\frac{G'_t}{G_t} = \frac{r_g}{r'_g} \cdot \frac{r'_g + R_0}{r_g + R_0} \qquad .. \quad .. \quad (3.9)$$

Similarly if R'_i is the resistive component of $Z_i(j\omega_0)$ corresponding to the value r'_g, it is easily shown that

$$\frac{R'_i}{R_i} = \frac{r'_g}{r_g} \cdot \frac{r_g + R_0}{r'_g + R_0} \qquad .. \quad .. \quad .. \quad (3.10)$$

and so $G'_t R' = G_t R_i$

All the preceding formulae refer to steady sinusoidal currents, but in connection with squegging, which is treated in Section 7, amplitude-modulated currents and voltages are encountered. Suppose that the modulated grid voltage of fundamental frequency is

$$v_{g1m} = V_{g1}(1 + p\cos\omega_s t)\cos\omega_0 t \quad .. \quad (3.11)$$

Then from (3.1) and (3.6) the corresponding anode voltage is

$$\begin{aligned} v_{a1m} &= Z_i(j\omega)\ Y_t(j\omega)\ v_{g1m} \\ &= -V_{a1}(1 + p\cos\omega_s t)\cos\omega_0 t \\ &+ V_{a1}\frac{X_i}{R_i}(1 + p\cos\omega_s t - 2pQ\frac{\omega_s}{\omega_0}\sin\omega_s t)\sin\omega_0 t \end{aligned}$$
$$.. \quad .. \quad .. \quad (3.12)$$

Of the two components of the anode voltage it is seen that the modulation on the first or in-phase component is not altered in any way in passing through the network. The modulation on the quadrature component, however, is altered both in phase and amplitude.

The anode current of fundamental frequency associated with the anode voltage given by (3.12) is $i_{a1m} = -Y_t(j\omega)\ v_{g1m}$

Substituting for $Y_t(j\omega)$ from (3.1) and for v_{g1m} from (3.11)

$$i_{a1m} = \frac{V_{a1}}{R_i}\left\{1 + p\cos\omega_s t - 2pQ\frac{\omega_s}{\omega_0}\sin\omega_s t\right\}\cos\omega_{0t} \quad .. \quad .. \quad .. \quad .. \quad (3.13)$$

This concludes the analysis of the feedback network.

Sometimes it is more convenient to connect the grid resistor R_g between 6 and 4, instead of in the position shown. The only effect of this change is to put an additional path for high-frequency currents between 6 and 4, without affecting in any other way the operation of the oscillator.

4. Grid Current

The object of this section is to calculate the grid current and thence the grid-bias voltage and the grid input resistance. If the alternating grid voltage is sinusoidal the work is simple, but there are two factors which give rise to harmonic grid voltages. Since the Q factor of the feedback network cannot be infinite, the harmonic anode and grid currents produce harmonic grid voltages, and, depending on the magnitude of these, the grid-bias voltage and the grid input impedance are more or less altered. The second factor is the time constant R_gC_g of the grid resistor and capacitor. Since this cannot be infinite the pulsating grid current produces harmonic grid voltages between 5 and 6.

To solve the problem, the method which has been adopted is to carry through the calculation, first on the assumption that Q and R_gC_g are infinitely large, and then to examine separately the effects of finite values of Q and R_gC_g. It is particularly important to find the minimum value of R_gC_g which will give satisfactory results, for the maximum value is limited by considerations of amplitude stability (squegging).

Let the mean grid current be I_g. This flows through R_g, and if the resistance to direct current between 3 and 4 is negligible compared with R_g the mean grid voltage is

$$-R_gI_g = V_g$$

Assuming Q and R_gC_g to be infinite, harmonic voltages are zero and the grid voltage can be written

$$v_g = V_{g1}\cos\omega_0 t + V_g \qquad .. \quad .. \quad (4.1)$$

It is found that in receiving valves and small

transmitting valves having unipotential oxide-coated cathodes the relation between grid current and grid voltage is approximately linear for small positive grid voltages, and varies but little with anode or screen voltage provided this is considerably greater than the grid voltage. If anode and grid voltages become comparable the grid current increases at a greater rate. This may happen if the anode load resistance R_i is large and the valve is driven hard. It will be supposed, however, that in the oscillators to which this analysis applies the excursion of the anode voltage is not a large fraction of the h.t. supply voltage.

When the grid voltage is negative the grid current characteristic is approximately exponential. This is important when very small values of oscillation amplitude have to be considered, and is discussed in Section 8 in connection with amplitude instability. Under normal steady-state conditions the oscillation amplitude is always large enough to make the linear law an accurate approximation.

The relation between grid current and voltage can then be written

$$\begin{aligned} i_g &= b_g (v_g - V_{cg}) \text{ if } v_g - V_{cg} > 0 \\ &= 0 \qquad\quad \text{if } v_g - V_{cg} < 0 \end{aligned} \quad \ldots \quad (4.2)$$

b_g and V_{cg} are constants peculiar to the valve.

Substituting for v_g according to (4.1) gives

$$i_g = b_g (V_{g1} \cos \omega_0 t + V_g - V_{cg})$$

and current flows when $V_{g1} \cos \omega_0 t + V_g - V_{cg} > 0$; e.g., from $\omega_0 t = -\phi$ to $\omega_0 t = \phi$ in the cycle centred on $t = 0$, where

$$\cos \phi = -\frac{(V_g - V_{cg})}{V_{g1}}$$

In practical oscillators V_g is much greater than V_{cg} and is comparable with V_{g1} so that current flows only for a fraction of each cycle.

The mean grid current is

$$I_g = \frac{b_g}{2\pi} \int_{-\phi}^{\phi} (V_{g1} \cos \theta + V_g - V_{cg})\, d\theta$$

From this and the preceding formula

$$\begin{aligned} -V_g = R_g I_g &= \frac{V_{g1} b_g R_g}{\pi} (\sin \phi - \phi \cos \phi) = \\ & V_{g1} \cos \phi - V_{cg} \end{aligned} \quad \ldots \quad (4.3)$$

$b_g R_g$ could be found from this equation in terms of V_g/V_{g1} and V_{cg}/V_{g1}, and graphs of V_g/V_{g1} versus $b_g R_g$ could be drawn for various values of V_{cg}/V_{g1}. A simpler, though approximate, method is to proceed as follows:

Let ϕ_0 be the value of ϕ corresponding to $V_{cg} = 0$. Let $\phi = \phi_0 + \delta$ and suppose that δ is so small that $\cos \delta = 1$ and $\sin \delta = \delta$. Then (4.3) becomes

$$\begin{aligned} V_{g1} \frac{b_g R_g}{\pi} (\sin \phi_0 - \phi_0 \cos \phi_0 + \phi_0 \delta \sin \phi_0) = \\ V_{g1} \cos \phi_0 - V_{g1} \delta \sin \phi_0 - V_{cg} \end{aligned}$$

Since $\phi = \phi_0$ when $V_{cg} = 0$

$$\frac{b_g R_g}{\pi} (\sin \phi_0 - \phi_0 \cos \phi_0) = \cos \phi_0 \quad \ldots \quad (4.4)$$

Substituting this into the above equation gives

$$V_{g1} \delta \sin \phi_0 = -V_{cg} (1 - \phi_0 \cot \phi_0) \ldots \quad (4.5)$$

Then

$$\begin{aligned} V_g &= -V_{g1} \cos \phi_0 + V_{g1} \delta \sin \phi_0 + V_{cg} \\ &= -V_{g1} \cos \phi_0 + V_{cg} \phi_0 \cot \phi_0 \ldots \end{aligned} \quad (4.6)$$

Fig. 2 shows $\cos \phi_0$ and $\phi_0 \cot \phi_0$ plotted against $b_g R_g$. Exact values for V_g calculated from (4.3) indicate that for the range of $b_g R_g$ covered by Fig. 2 the error in formula (4.6) is less than about 1 % for values of V_{cg}/V_{g1} between 0.3 and −0.6. In practice the values of V_{cg}/V_{g1} are negative and much less numerically than 0.6.

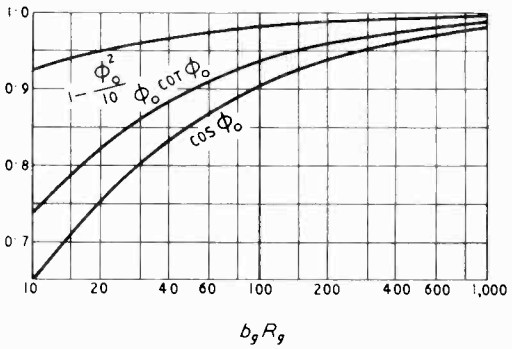

Fig. 2. *Graphs of the grid-bias and grid-resistance functions.*

Next consider the amplitude I_{g1} of the component of fundamental frequency in i_g. This is

$$\begin{aligned} I_{g1} &= \frac{b_g}{\pi} \int_{-\phi}^{\phi} (V_{g1} \cos \theta + V_g - V_{cg}) \cos \theta \, d\theta \\ &= \frac{b_g V_{g1}}{\pi} (\phi - \sin \phi \cos \phi) \\ &= \frac{2}{3} \cdot \frac{b_g}{\pi} V_{g1} \phi^3 (1 - \phi^2 + \cdots) \end{aligned}$$

Similarly from (4.3)

$$I_g = \frac{b_g}{3} \cdot \frac{V_{g1}}{\pi} \phi^3 \left(1 - \frac{\phi^2}{10} + \cdots\right)$$

$$\therefore I_{g1} = 2 I_g \left(1 - \frac{\phi^2}{10} + \cdots\right) \quad \ldots \quad (4.7)$$

The grid input resistance at fundamental frequency is

$$\begin{aligned} r_g = \frac{V_{g1}}{I_{g1}} &= \frac{V_{g1}}{2 I_g} \Big/ \left(1 - \frac{\phi^2}{10} + \cdots\right) \\ &= -\frac{R_g}{2} \cdot \frac{V_{g1}}{V_g} \Big/ \left(1 - \frac{\phi^2}{10} + \cdots\right) \end{aligned}$$

Since ϕ is not very different from ϕ_0 and the term $1-\phi^2/10$ is in any case small, it is permissible to write

$$r_g = -\frac{R_g}{2}\cdot\frac{V_{g1}}{V_g}\left|\left(1-\frac{\phi^2_0}{10}\right)\right. \quad .. \quad .. \quad (4.8)$$

The value of $1-\phi^2/10$ is shown in Fig. 2 It is only at the smallest values of b_gR_g that this term is appreciably different from 1. In most examples the difference can be neglected.

Now suppose that R_gC_g is still infinite, but that, because of the finite value of Q, the grid voltage contains harmonic components, and that the mean grid voltage is thereby altered to $V_g + \delta V_g$. Then from (3.4)

$$v_g = V_{g1}\cos\omega_0 t + \sum_2^\infty V_{gn}\sin n\omega_0 t + V_g + \delta V_g$$

The grid current is

$$i_g = b_g\left(V_{g1}\cos\omega_0 t + V_g - V_{cg} + \sum_2^\infty V_{gn}\sin n\omega_0 t + \delta V_g\right)$$

It will be assumed that V_{cg} is zero, so that $\phi = \phi_0$. The effect of V_{cg} on the value of δV_g can be shown to be negligibly small. Let conduction now begin when $\omega_0 t = -(\phi_0 + \delta_1)$ and end when $\omega_0 t = \phi_0 + \delta_2$. Then

$$V_{g1}\cos(\phi_0+\delta_1) - V_{g1}\cos\phi_0 - \sum_2^\infty V_{gn}\sin n(\phi_0+\delta_1) + \delta V_g = 0.$$

Assuming that $\sum_2^\infty V_{gn}\sin n\phi_0$ is small and δ_1 is so small that $\sin\delta_1 = \delta_1$ and $\cos\delta_1 = 1 - \delta_1^2/2$

$$\tfrac{1}{2}\delta_1^2\left(V_{g1}\cos\phi_0 - \sum_2^\infty V_{gn}\sin n\phi_0\right) + \delta_1\left(V_{g1}\sin\phi_0 + \sum_2^\infty nV_{gn}\cos n\phi_0\right) + \sum_2^\infty V_{gn}\sin n\phi_0 - \delta V_g = 0.$$

From which

$$\delta_1\left(V_{g1}\cos\phi_0 - \sum_2^\infty V_{gn}\sin n\phi_0\right) = -\left(V_{g1}\sin\phi_0 + \sum_2^\infty nV_{gn}\cos n\phi_0\right) + \left\{\left(V_{g1}\sin\phi_0 + \sum_2^\infty nV_{gn}\cos n\phi_0\right)^2 + 2\left(V_{g1}\cos\phi_0 - \sum_2^\infty V_{gn}\sin n\phi_0\right)\left(\delta V_g - \sum_2^\infty V_{gn}\sin n\phi_0\right)\right\}^{\frac{1}{2}} \quad .. \quad .. \quad .. \quad (4.9)$$

The expression for δ_2 is obtained from this by writing $-V_{gn}$ in place of V_{gn}

The mean grid current is

$$I_g + \delta I_g = I_g - \delta V_g/R_g = \frac{b_g}{2\pi}\int_{-\phi_0-\delta_1}^{\phi_0+\delta_0}\left(V_{g1}\cos\theta + V_g + \sum_2^\infty V_{gn}\sin n\theta + \delta V_g\right)d\theta$$

$$= I_g - \frac{b_g}{4\pi}\left[V_{g1}(\delta_1^2+\delta_2^2)\sin\phi_0 + 2(\delta_1-\delta_2)\sum_2^\infty V_{gn}\sin n\phi_0 + (\delta_1^2-\delta_2^2)\sum_2^\infty nV_{gn}\cos n\phi_0 - 2\delta V_g(2\phi_0+\delta_1+\delta_2)\right]$$

$$\therefore \delta V_g\left\{\left(1+\frac{b_gR_g\phi_0}{\pi}\right)+\frac{b_gR_g}{2\pi}(\delta_1+\delta_2)\right\} = \frac{b_gR_g}{4\pi}\left[V_{g1}(\delta_1^2+\delta_2^2)\sin\phi_0 + 2(\delta_1-\delta_2)\sum_2^\infty V_{gn}\sin n\phi_0 + (\delta_1^2-\delta_2^2)\sum_2^\infty nV_{gn}\cos n\phi_0\right]$$

From (4.4) $1 + \frac{b_gR_g\phi_0}{\pi} = \frac{b_gR_g}{\pi}\tan\phi_0$

$$\therefore \frac{\delta V_g}{V_g}\{\sin\phi_0 + \tfrac{1}{2}(\delta_1+\delta_2)\cos\phi_0\} = \tfrac{1}{4}\{2(\delta_2-\delta_1)\sum_2^\infty\frac{V_{gn}}{V_{g1}}\sin n\phi_0 + (\delta_2^2-\delta_1^2)\sum_2^\infty n\frac{V_{gn}}{V_{g1}}\cos n\phi_0 - (\delta_2^2+\delta_1^2)\sin\phi_0\}$$

Since δV_g is involved in the expressions for δ_1 and δ_2 this equation cannot be solved directly for δV_g. The method which has been adopted is to calculate δ_1 and δ_2 from (4.9) on the assumption that $\delta V_g/V_g$ has certain small values (e.g., 1%, 2%) and to find the values of $\delta V_g/V_g$ given by the above equation using these values of δ_1 and δ_2. The calculated values of $\delta V_g/V_g$ are then plotted against the assumed values, and the point at which they are equal is the true value of $\delta V_g/V_g$.

The effect of the harmonic voltages increases slightly as b_gR_g increases, but it is always very small. As an example, consider the extreme case in which $b_gR_g = 1000$, and the amplitudes of the second and third harmonic voltages are 5% and 3%, higher harmonics being negligible. The corresponding value of $\delta V_g/V_g$ is 1.6%. In practice the value of b_gR_g is usually much less than 1000, and the harmonic voltages are seldom as great as the values assumed. It can be shown similarly that the effect of the harmonic voltages on the grid input impedance is also negligible.

The effect of a finite value of R_gC_g can now be considered. It will be supposed that the Q factor of the oscillatory circuit is infinite so that the voltage between 3 and 4 is sinusoidal. The pulsating grid current, however, produces a non-sinusoidal voltage between 5 and 6 which changes the mean grid voltage and the grid input impedance. Another effect of a non-

infinite value for R_gC_g is a small change in the amplitude and phase of the fundamental grid voltage. The aim of the following calculation is to find the value of V_g corresponding to any given value of R_gC_g, and thence to find the values of R_gC_g which produce certain specified small changes in the value of the mean grid voltage.

Let the voltage between 3 and 4 be v_3. For

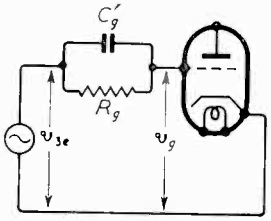

Fig. 3. *Equivalent circuit for grid-current calculation.*

the purpose of calculating the grid current the part of the feedback network to the right of terminals 3 and 4 may be replaced, according to Thévenin's theorem, by the equivalent circuit shown in Fig. 3 in which

$$C'_g = C_g + c_{gk}$$

and $$v_{3e} = v_3 \frac{1 + j\omega_0 C_k R_g}{1 + j\omega_0 C'_g R_g}$$

In practical oscillators R_g is many times $1/\omega_0 C_g$ and C_g is several times c_{gk}. Then to a high degree of accuracy

$$v_{3e} = v_3 \frac{C_g}{C'_g}$$

For example, if C_g is 5 times c_{gk} and R_g is 15 times $1/\omega_0 C_g$ the error in V_{3e} is only 0.07% and the phase error only 0.01 radian.

It is assumed initially that V_{cg} is zero. The effect of a finite V_{cg} is considered later and is shown to be small.

Let $v_{3e} = V_{3e} \cos \omega_0 t$

Let v_b be the instantaneous value of the voltage across C'_g, and let grid current begin, in the cycle centered on $t = 9$, when $\omega_0 t = -\phi_1$ and end when $\omega_0 t = \phi_2$. In the following cycle grid current begins when $\omega_0 t = 2\pi - \phi_1$.

During the conduction period the grid current is

$$i_g = b_g (V_{3e} \cos \omega_0 t + v_b)$$

This must be equal to the sum of the currents flowing through R_g and C'_g, which is

$$-\frac{v_b}{R_g} - C'_g \frac{dv_b}{dt}$$

$$\therefore \quad \frac{C'_g}{b_g} \cdot \frac{dv_b}{dt} + v_b\left(1 + \frac{1}{b_g R_g}\right) = -V_{3e} \cos \omega_0 t$$

This differential equation is of simple and well-known type. The solution is easily found to be

$$v_b = a \exp(-pb_g X_g \omega_0 t) - \frac{V_{3e} \sin \alpha}{p} \sin(\omega_0 t + \alpha) \quad .. \quad .. \quad .. \quad .. \quad .. \quad .. \quad (4.10)$$

in which

$$\left.\begin{aligned} p &= 1 + 1/b_g R_g \\ \tan \alpha &= p\, b_g X_g \\ X_g &= 1/\omega_0 C'_g \end{aligned}\right\} \quad .. \quad .. \quad .. \quad (4.11)$$

and a is a constant determined by the initial conditions. The grid current, and therefore $V_{3e} \cos \omega_0 t + v_b$, is zero when $\omega_0 t = -\phi_1$ and when $\omega_0 t = \phi_2$. Applying these conditions to (4.10) gives

$$\left.\begin{aligned} a \exp(pb_g X_g \phi_1) &= \frac{V_{3e} \sin \alpha}{p} \sin(-\phi_1 + \alpha) - V_{3e} \cos \phi_1 \\ a \exp(-pb_g X_g \phi_2) &= \frac{V_{3e} \sin \alpha}{p} \sin(\phi_2 + \alpha) - V_{3e} \cos \phi_2 \end{aligned}\right\} \quad (4.12)$$

Let $\phi_1 + \phi_2 = 2\phi_s$ and $\phi_1 - \phi_2 = 2\phi_d$.

Two new equations may be formed by subtracting and adding the corresponding sides of equations (4.12), and the quotients of the corresponding sides of these new equations form a third equation, which, after substituting for ϕ_1 and ϕ_2, may be written

$$\tanh(pb_g X_g \phi_s) =$$

$$\frac{p \sin \phi_d \sin \phi_s - \sin \alpha \cos(\alpha - \phi_d) \sin \phi_s}{\sin \alpha \sin(\alpha - \phi_d) \cos \phi_s - p \cos \phi_d \cos \phi_s}$$

$$= \tan \phi_s \left[\frac{\sin \alpha \cos \alpha - (p - \sin^2 \alpha) \tan \phi_d}{\sin \alpha \cos \alpha \tan \phi_d + p - \sin^2 \alpha}\right]$$

$$= \tan \phi_s \left[\frac{1 - q \tan \phi_d}{q + \tan \phi_d}\right]$$

where $$q = \frac{p - \sin^2 \alpha}{\sin \alpha \cos \alpha} = \frac{1}{b_g X_g} + \frac{pX_g}{R_g} \quad .. \quad (4.13)$$

The above equation may be rewritten as

$$\tan \phi_d = \frac{\tan \phi_s - q \tanh(pb_g X_g \phi_s)}{q \tan \phi_s + \tanh(pb_g X_g \phi_s)} \quad (4.14)$$

Between the end of one conducting period at $\omega_0 t = \phi_2$ and the beginning of the next at $\omega_0 t = 2\pi - \phi_1$, C'_g discharges exponentially through R_g. During this time

$$v_b = d \exp\left(-\frac{X_g \omega_0 t}{R_g}\right) \quad .. \quad .. \quad (4.15)$$

where d is a constant determined by the initial conditions. At the beginning and end of the discharge period $V_{3e} \cos \omega_0 t + v_b$ is zero.

$$\left.\begin{aligned} \therefore\ d \exp\left(-\frac{X_g \phi_2}{R_g}\right) &= -V_{3e} \cos \phi_2 \\ d \exp\left(\frac{X_g(\phi_1 - 2\pi)}{R_g}\right) &= -V_{3e} \cos \phi_1 \end{aligned}\right\} \quad (4.16)$$

By subtracting and adding the corresponding sides of these equations, and taking the quotients

of the corresponding sides of the two new equations thus formed, one obtains

$$\tan \phi_d = \cot \phi_s \tanh \left\{ \frac{X_g(\pi - \phi_s)}{R_g} \right\} \quad (4.17)$$

and $\tan \phi_d$ may be eliminated between (4.14) and (4.17) to give an equation containing ϕ_s only,

$$\tanh \left\{ \frac{X_g(\pi - \phi_s)}{R_g} \right\} [q \tan \phi_s + \tanh (p b_g X_g \phi_s)] = \tan \phi_s [\tan \phi_s - q \tanh (p b_g X_g \phi_s)]$$

This equation could be solved graphically, but an approximate analytical solution is less laborious and more accurate. A rough approximation for ϕ_s is ϕ_o, which can be found from Fig. 2. By Newton's method of successive approximations the value of ϕ_s can then be calculated to any required degree of accuracy. ϕ_d follows at once from (4.17).

The mean value of the grid voltage can now be calculated. This is done by integrating v_b over a cycle of oscillation. Expression (4.10) is integrated between $\omega_o t = -\phi_1$ and $\omega_o t = \phi_2$ and expression (4.15) between $\omega_o t = \phi_2$ and $\omega_o t = 2\pi - \phi_1$. When the exponential terms have been eliminated by substitution from (4.12) and (4.16) the solution, denoted by V'_g, can be written

$$V'_g = -\frac{V_{3e}}{\pi} \left[\frac{R_g}{X_g} \left(1 - \frac{1}{p b_g R_g} \right) \sin \phi_s \sin \phi_d + \frac{\sin \alpha \sin \phi_s}{p} \left\{ \sin (\alpha - \phi_d) + \frac{1}{p b_g X_g} \cos (\alpha - \phi_d) \right\} \right]$$

On substituting for α and p according to (4.11) this becomes

$$V'_g = -\frac{V_{3e} \sin \phi_s}{p\pi} \left[\cos \phi_d + \frac{R_g}{X_g} \sin \phi_d \right]$$

If R_g/X_g were infinite the mean grid voltage would be

$$V_g = -V_{3e} \cos \phi_o$$

Hence

$$\frac{V'_g}{V_g} = \frac{\sin \phi_s \cos \phi_d}{p\pi \cos \phi_o} \left[1 + \frac{R_g}{X_g} \tan \phi_d \right] \quad (4.18)$$

In Fig. 4 are shown the values of $b_g R_g$ and R_g/X_g which correspond to values of $1 - V'_g/V_g$ of 0.5%, 1% and 2%.

This problem has also been studied by Marique[2] whose method was to find ϕ_1 and ϕ_2 by solving graphically two simultaneous equations in ϕ_1 and ϕ_2. Marique also assumed that the mean value of v_b during the charging period is equal to the mean value during the discharge period. In spite of these limitations the values of V'_g obtained by Marique are in good agreement with those calculated from the exact formulae developed in this Section. Marique gave a table of values of $b_g R_b$ and corresponding value of $R_b/2\pi X_b$ beyond which no appreciable increase in the bias voltage occurs as the value of X_b is reduced. The points corresponding to these values lie between the 0.5% and the 1% graphs of Fig. 4.

The effect of the grid-current cut-off voltage V_{cg}, which so far has been neglected, can now be considered. It can be seen from (4.2) that, so far as the grid current is concerned, V_{cg} has the same effect as a generator of e.m.f. $-V_{cg}$, with zero impedance, connected in series with the grid.

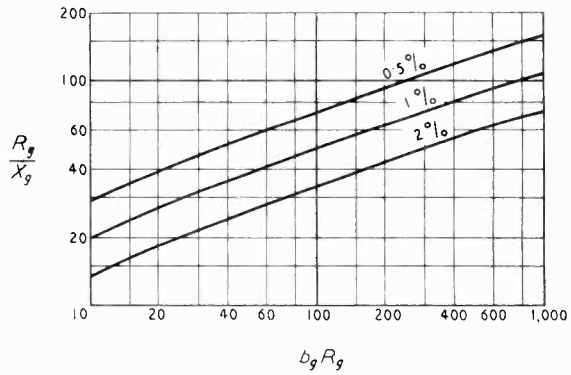

Fig. 4. *Percentage decrease in grid-bias voltage.*

Suppose that for any particular values of R_g, C_g, and V_{cg}, the mean grid current is I_g. The mean grid current would be unchanged if the generator were removed and replaced by a resistor of value V_{cg}/I_g shunted by a very large capacitor. Since the alternating grid current flows almost entirely through the grid capacitor, the two resistors and two capacitors could be replaced, with little effect on the grid current, by a single resistor of value $R_g + V_{cg}/I_g = R_g(1 - V_{cg}/V_g)$ shunted by a capacitor of value C_g. It is concluded that for the small changes of V_g which are of interest the graphs of Fig. 4 are valid if R_g is replaced by $R_g(1 - V_{cg}/V_g)$, but it is obvious from inspection of the graphs that this makes a negligible difference to the values of X_g.

Finally the effect of a finite time-constant on the grid input impedance can be calculated. The grid current of fundamental frequency can be expressed as

$$I_{g1c} \cos \omega_o t + I_{g1s} \sin \omega_o t$$

or symbolically $(I_{g1c} - jI_{g1s}) \exp j\omega_0 t$

where $I_{g1c} = \frac{b_g}{\pi} \int_{\phi_1}^{\phi_2} (V_{3e} \cos \theta + v_b) \cos \theta \, d\theta$

v_b is given by (4.10). The integral is equal to

$$I_{g1c} = \frac{V_{3e}}{\pi} \frac{b_g}{(1 + p^2 b_g^2 X_g^2)} \left[\sin \phi_s \cos \phi_s \left\{ \left(\frac{2X_g}{R_g} + b_g X_g \right) \sin 2\phi_d - \left(1 - \frac{X_g^2}{R_g^2} - \frac{b_g X_g^2}{R_g} \right) \cos 2\phi_d \right\} + \phi_s \left(1 + \frac{X_g^2}{R_g^2} + \frac{b_g X_g^2}{R_g} \right) \right]$$

Similarly

$$I_{g1s} = \frac{V_{3e}\, b_g}{\pi(1 + p^2 b^2_g X^2_g)}\left[\sin\phi_s \cos\phi_s \left\{\left(1 - \frac{X^2_g}{R^2_g} - \frac{b_g X^2_g}{R_g}\right)\sin 2\phi_d + \left(\frac{2X_g}{R_g} + b_g X_g\right)\cos 2\phi_d\right\} - b_g X_g \phi_s\right]$$

The grid voltage of fundamental frequency is

$$\left\{V_{3e} + \frac{jR_g X_g}{R_g - jX_g}(I_{g1c} - jI_{g1s})\right\}\exp j\omega_0 t$$

Hence the grid input impedance is

$$z_g = \frac{V_{3e}}{I_{g1c} - jI_{g1s}} + \frac{jR_g X_g}{R_g - jX_g} = r_g + jx_g$$

It is found that for the values of $b_g R_g$ and R_g/X_g shown in Fig. 4 the values of r_g do not differ from the values corresponding to an infinite $R_g C_g$ by percentages greater than those shown in Fig. 4 for the change in V_g, and that x_g is always a small fraction of r_g. If it is assumed that errors in V_g and r_g less than say 10% can be neglected, then formulae (4.6) and (4.8) can be used, provided R_g/X_g is greater than the value shown in Fig. 4 corresponding to the assumed error.

5. Anode Current

The anode current in a valve is the difference between the cathode current and the sum of the currents flowing to all the other electrodes. Thus for triodes

$$i_a = i_k - i_g$$

In a triode the cathode current may be represented fairly accurately, over a certain range, by the expression

$$i_k = b_a (v_g + v_a/\mu)^{\frac{3}{2}} \text{ if } v_g + v_a/\mu > 0$$
$$= 0 \qquad \text{if } v_g + v_a/\mu < 0$$

in which v_a is the anode voltage and b_a and μ are constants peculiar to the valve. μ is the amplification factor. The errors in this formula occur mainly at large and small values of i_k. At large values, i_k may show a saturation effect, but this does not happen with oxide-coated cathodes under normal conditions. Errors at large values of i_k may also arise if the grid voltage is positive and the anode voltage is lowered to a value comparable with v_g. This may happen if the anode-lead impedance R_i is large and the valve is driven hard. It will be supposed, however, that in the oscillators to which this analysis applies the anode alternating voltage is not a very large fraction of the h.t. supply voltage.

At small values of i_k errors may be produced by the fringing of the electrostatic field at the extremities of the electrodes, by the initial velocity of the electrons and other effects. Discrepancies at small values of i_k are comparatively innocuous.

Under operating conditions v_a is the sum of a constant component V_a, (the h.t. supply voltage) and an alternating component v_{aa}.

$$\therefore i_a = b_a (v_g + v_{aa}/\mu - V_{ca})^{\frac{3}{2}} - i_g$$

where V_{ca} is the value of v_g at which i_k becomes zero under static conditions; i.e., when v_{aa} is zero. V_{ca} is always negative and is referred to as the anode current cut-off voltage.

In tetrode and pentode valves the anode current bears an almost constant ratio to the screen current provided the anode voltage is not too low, Let the anode current be k times and the screen current $1-k$ times the sum of these currents. For most valves k is of the order of 0.75. If the screen voltage is fixed the expression for the anode current is similar to that given above for triodes.

$$\therefore i_a = b_a (v_g + v_{aa}/\mu - V_{ca})^{\frac{3}{2}} - k i_g \quad (5.1)$$

The constant b_a here refers, of course, to the anode current and not to the cathode current. This expression may serve for all kinds of valves. For triodes $k=1$. For tetrodes and pentodes μ is usually so large that v_{aa}/μ can be neglected, and k may be taken as 0.75 if the true value is not known.

Taking account of harmonics, the grid voltage is $v_g = V_{g1}\cos\omega_0 t + V_g + \sum_2^\infty V_{gn}\sin n\omega_0 t$

and the alternating anode voltage is

$$v_{aa} = -V_{a1}\cos\omega_0 t + \frac{V_{a1}X_i}{R_i}\sin\omega_0 t + \sum_2^\infty V_{an}\sin n\omega_0 t$$

Substituting these expressions into (5.1) and expanding by Taylor's theorem

$$i_a = b_a\{(V_{g1} - V_{a1}/\mu)\cos\omega_0 t + V_g - V_{ca}\}^{\frac{3}{2}} - k i_g + \frac{3}{2} b_a \left\{\frac{V_{a1}X_i}{\mu R_i}\sin\omega_0 t + \sum_2^\infty (V_{gn} + V_{an}/\mu)\sin n\omega_0 t\right\} \{(V_{g1} - V_{a1}/\mu)\cos\omega_0 t + V_g - V_{ca}\}^{\frac{1}{2}}$$

In the absence of the quadrature anode voltage $V_{a1}\frac{X_i}{R_i}\sin\omega_0 t$ and of the harmonic voltages, i_a could be represented by the series

$$I_a + \sum_1^\infty I_{an}\cos n\omega_0 t.$$

It is seen from the preceding expression for i_a that, since the values of $\frac{V_{a1}X_i}{\mu R_i}$ and $V_{gn} + \frac{V_{an}}{\mu}$ are all small compared with V_{g1}, the effect of

adding the quadrature and harmonic voltages is to produce additional currents of small amplitudes in phase quadrature with the existing currents. These extra currents have therefore a negligible effect on the amplitudes and only a small effect on the relative phases of the total currents. The main result of the quadrature and harmonic voltages is a slight change in the frequency of oscillation.

The amplitude of the component of fundamental frequency in i_a is therefore

$$I_{a1} = \frac{b_a}{\pi}\int_{-\pi}^{\pi}\left\{(V_{g1}-V_{a1}/\mu)\cos\theta + V_g - V_{ca}\right\}^{\frac{3}{2}} \cos\theta\, d\theta - \frac{kV_{g1}}{r_g}$$

where V_{g1}/r_g is the amplitude of the fundamental component in the grid current. The integral is evaluated in the Appendix. Two cases exist depending on whether $V_{g1}-V_{a1}/\mu$ is greater or less than $V_g - V_{ca}$.

If $V_{g1}-V_{a1}/\mu < V_g - V_{ca}$ anode current flows continuously, and the result of integration is

$$I_{a1} = \frac{3}{2}\, b_a\left(V_{g1}-V_{a1}/\mu\right)\left(V_g-V_{ca}\right)^{\frac{1}{2}} \left\{1 - \frac{(V_{g1}-V_{a1}/\mu)^2}{32(V_g-V_{ca})^2} - \ldots\right\} - \frac{kV_{g1}}{r_g} \quad \ldots \quad (5.2)$$

The terms in the series diminish rapidly and higher terms may be neglected.

From (3.2) $I_{a1} = -G_t V_{g1}$ and from (3.7) $V_{a1} = -G_t R_t V_{g1}$

Let $$N = -\frac{3}{2}\cdot\frac{b_a}{G_t}\cdot\frac{(1+G_tR_i/\mu)(-V_{ca})^{\frac{1}{2}}}{1-k/G_t r_g} \quad (5.3)$$

$$K = -\frac{V_g}{V_{g1}}\cdot\frac{1}{1+G_tR_i/\mu} \quad \ldots \quad (5.4)$$

Then (5.2) can be written in the form

$$1 = N\left(1-V_g/V_{ca}\right)^{\frac{1}{2}}\left\{1 - \frac{1}{32K^2(1-V_{ca}/V_g)^2}\right\} \quad (5.5)$$

If $V_{g1}-V_{a1}/\mu > V_g - V_{ca}$ anode current flows only when $-\beta < \omega_o t < \beta$ where

$$\cos\beta = \frac{-(V_g - V_{ca})}{V_{g1}(1+G_tR_i/\mu)} = K\left(1-V_{ca}/V_g\right)$$

The result of integration is then

$$I_{a1} = \frac{3b_a}{2^{\frac{1}{2}}}V_{g1}^{\frac{3}{2}}\left(1+G_tR_i/\mu\right)^{\frac{3}{2}}\sin^4\frac{\beta}{2}\left\{1 - \frac{1}{4}\sin^2\frac{\beta}{2} - \frac{5}{128}\sin^4\frac{\beta}{2}\right\} - \frac{kV_{g1}}{r_g} \quad (5.6)$$

Higher terms can be neglected

Substituting for N, K and I_{a1} as above, (5.6) becomes

$$I = \frac{N}{2^{\frac{3}{2}}}\left(\frac{V_g}{KV_{ca}}\right)^{\frac{1}{2}}H^2\left(1 - \frac{H}{8} - \frac{5H^2}{512}\right) \quad \ldots \quad (5.7)$$

where $$H = 2\sin^2\frac{\beta}{2} = 1 - K + \frac{KV_{ca}}{V_g} \quad \ldots \quad (5.8)$$

From (5.5) and (5.7) N can be found in terms of V_g/V_{ca} and K. Fig. 5 shows V_g/V_{ca} plotted as a function of N for several values of K. The method of using Fig. 5 to calculate the oscillation amplitude is explained in the next Section.

If the graphs were continued upwards it would be found that for all values of K less than 1 there is a point on each graph at which its slope becomes infinite and thereafter negative. This behaviour is investigated in Section 8 where it is shown that all values of V_g/V_{ca} greater than these critical values correspond to unstable states.

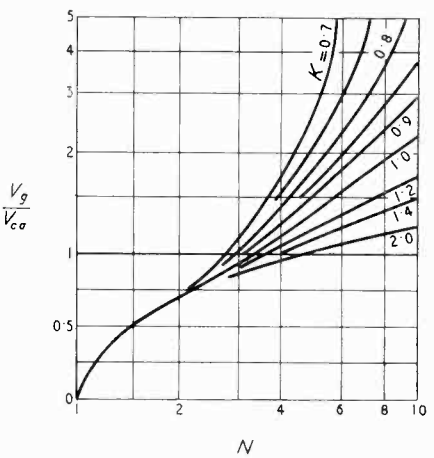

Fig. 5. *Graphs for the grid-bias voltage.*

For design purposes it is useful to know the mean anode current. This is

$$I_a = \frac{b_a}{2\pi}\int_{-\pi}^{\pi}\{V_{g1}(1 + G_tR_i/\mu)\cos\theta + V_g - V_{ca}\}^{\frac{3}{2}}\, d\theta + \frac{kV_g}{R_g}$$

From the integral evaluated in the Appendix,

if $V_{g1}\left(1 + \frac{G_tR_i}{\mu}\right) < V_g - V_{ca}$

$$I_a = b_a(V_g - V_{ca})^{\frac{3}{2}}\left\{1 + \frac{3}{16K^2(1 - V_{ca}/V_g)^2}\right\} + \frac{kV_g}{R_g}$$

If $V_{g1}(1 + G_tR_i/\mu) > V_g - V_{ca}$

$$I_a = \frac{3b_a}{2^{\frac{3}{2}}} V_{g1}^{\frac{3}{2}} (1 + G_tR_i/\mu)^{\frac{3}{2}} \sin^4\frac{\beta}{2} \left\{1 + \frac{1}{12}\sin^2\frac{\beta}{2} + \frac{3}{128}\sin^4\frac{\beta}{2}\right\} + \frac{kV_g}{R_g} \quad (5.9)$$

Now $r_g \approx -\frac{R_g}{2}\cdot\frac{V_{g1}}{V_g}$ and kV_g/R_g is small compared with I_a, which may therefore be written with little error as

$$I_a = \frac{1}{2} I_{a1}\left(1 + \frac{H}{6} + \frac{7H^2}{192}\right) = -\frac{V_{g1}G_t}{2}\left(1 + \frac{H}{6} + \frac{7H^2}{192}\right) \quad (5.10)$$

In order to calculate the grid harmonic voltages the amplitudes of the anode harmonic currents are required. The two of most interest are the second and third. Neglecting grid current, the amplitude of the second harmonic current in i_a is

$$I_{a2} = \frac{b_a}{\pi}\int_{-\pi}^{\pi} \{V_{g1}(1 + G_tR_i/\mu)\cos\theta + V_g - V_{ca}\}^{\frac{3}{2}} \cos 2\theta\, d\theta$$

It is usually only for large values of oscillation amplitude that harmonic voltages have appreciable magnitudes, and so only the case in which $V_{g1}\left(1 + \frac{G_tR_i}{\mu}\right) > V_g - V_{ca}$ need be considered.

Then $I_{a2} = \frac{3b_a}{2^{\frac{1}{2}}} V_{g1}^{\frac{3}{2}} (1 + G_tR_i/\mu)^{\frac{3}{2}} \sin^4\frac{\beta}{2} \left\{1 - \frac{5}{4}\sin^2\frac{\beta}{2} + \frac{35}{128}\sin^4\frac{\beta}{2}\right\}$

$$\approx -V_{g1}G_t\left(1 - \frac{H}{2} + \frac{H^2}{64}\right) \quad (5.11)$$

Similarly

$$I_{a3} \approx -V_{g1}G_t\left(1 - \frac{4H}{3} + \frac{85H^2}{192} - \frac{H^3}{96}\right) \quad (5.12)$$

6. Method of Calculation and Example

The first step towards calculating the oscillation amplitude V_{g1} is to find the valve constants b_a, V_{ca}, b_g, V_{cg} and μ if these are not already known. This can be done most conveniently by graphical methods.

To find b_a and V_{ca}, the two-thirds power of the anode current is plotted for negative values of grid voltage, the screen and/or anode voltage being kept constant at its normal mean value. A straight line is drawn through the points ignoring the deviation from linearity at small values of i_a. The intercept of this line on the voltage axis is equal to V_{ca}, and $b_a = I_o(-V_{ca})^{-\frac{3}{2}}$ where I_o is the value of i_a when $v_g = 0$. Strictly a correction should be made for the grid current, but even when $v_g = 0$ this is a very small fraction of the anode current and may safely be neglected. Usually it is sufficient to plot three points which may conveniently be those corresponding to currents of about 100%, 60% and 20% of I_o. To avoid confusion it is best to express the values of the currents in amperes.

b_g and V_{cg} are found by plotting the grid current for small positive values of grid voltage, say up to about $V_{ca}/3$. A straight line is drawn through the points, ignoring deviations from linearity, particularly near to $v_g = 0$. The slope of this line is b_g and the intercept on the voltage axis is V_{cg}. The values of grid current should be those obtained when the normal anode and screen voltages are applied.

μ will usually be known, but if not it may be obtained by finding the ratio of anode and grid voltage changes which produce the same change in the anode current. This should also be done at the normal operating voltages as μ is not quite constant.

The constants G_t and R_i of the feedback network should next be evaluated. R_i is the resistive component of the impedance between 1 and 2 and G_t is the transfer conductance between 1, 2 and 6, 4 at the oscillation frequency. In calculating G_t and R_i account should be taken of the interelectrode capacitance of the valve and the grid input resistance.

To find the grid input resistance from (4.8) it is necessary first to find from (4.6) the value of V_g/V_{g1}, which in turn depends on the value of V_{cg}/V_{g1} which is not yet known. However, V_{cg}/V_{g1} is always small, so that a good approximation to the true value of V_g/V_{g1} can be obtained by assuming a rough value for V_{cg}/V_{g1}. A reasonable guess is $V_{cg}/V_{g1} = -V_{cg}/V_{ca}$. Approximate values for r_g, R_i, and G_t can then be calculated. N and K are found from (5.3) and (5.4). If the valve is a tetrode or pentode the value of k in (5.3) may be taken as 0.75. For triodes $k = 1$. V_g/V_{ca} is read off from Fig. 5 and so V_{g1} can be calculated, using the previously found value of V_g/V_{g1}.

An approximate value for V_{g1} having been obtained in this way, more accurate values for V_g/V_{g1}, N and K can be calculated, and, by repeating the procedure described above, a better approximation for V_{g1} may be found. This does not differ much from the first approximation so further approximations are unnecessary.

Should the grid harmonic voltages be of interest their approximate amplitudes can be found from (3.5), (5.11), and (5.12). The amplitude of the anode voltage of fundamental frequency is $V_{a1}(1 + X_i^2/R_i^2)^{\frac{1}{2}}$. It may be assumed that

when V_{a1} is large enough to be of interest X_i is negligible compared with R_i. Also $V_{a1} = -G_t R_i V_{g1}$ and the mean anode current is given by (5.9) or (5.10).

A check should be made to ensure that the assumptions on which the analysis is based are valid. The ratio R_g/X_g should be at least as great as the value shown by the 1% graph of Fig. 4. If the anode alternating voltage is a large fraction of the h.t. supply voltage the maximum grid voltage $V_g + V_{g1}$ and the minimum anode voltage $V_a + G_t R_i V_{g1}$ should be calculated. If the corresponding point lies above the 'knee' on the characteristic curves for the valve, (i.e., the region where the anode current begins to change very rapidly with the anode voltage), the calculated value of V_{g1} will be reasonably accurate. If the point lies below the 'knee' this is indicative of a poor design, as, in general, operation under such condition results in excessive grid or screen current. In such circumstances the assumptions made in the analysis are not accurate.

Two general conclusions may be drawn from the graphs of Fig. 5. If a large amplitude is required K should be small. This implies that the grid resistance R_g and the anode load resistance R_i should be small. On the other hand if good regulation (i.e., constancy of amplitude with respect to changes of load) is more important, both these quantities should be large.

Example: The following data apply to the triode section of a triode-hexode frequency-changer valve: $b_g = 0.00065$, $V_{cg} = -0.13$, $b_a = 0.00056$, $V_{ca} = -9.1$, $\mu = 20$. The feedback network consists of a parallel resonant circuit connected between 1 and 2 and a coupling coil of negligible resistance connected between 3 and 4. Coupling between grid and anode circuits is provided by a mutual inductance between the two coils which has a value -0.5 times the inductance of the anode coil, and the coefficient of coupling may be taken as 1.

$$R_g = 10^5\ ;\ C_g = 10^{-7}\ ;$$

the frequency of oscillation is 1 kc/s. (Note.—All these quantities are expressed in terms of practical units—volts, amperes, ohms and farads).

Find the oscillation amplitude when the dynamic resistance of the resonant circuit by itself (i.e., with the power supplies to the valve cut off) has the values 10,000, 5,000 and 2,500 ohms.

From the data $b_g R_g = 65$ and $V_{cg}/V_{ca} = 0.014$. From (4.6) and Fig. 2 the first approximation to V_g/V_{g1} is -0.89, and from (4.8) the grid input resistance is 57,600 Ω. When the dynamic resistance of the resonant circuit is 10,000 Ω the network input resistance R_i is equal to a resistance of 10,000 Ω in parallel with a resistance of $57{,}600 \times 0.5 = 230{,}400$ Ω; therefore $R_i = 9580$Ω and $G_t = -2/9580 = -0.000209$ mho. From (5.3.) and (5.4.) $N = 10.1$ and $K = 0.99$. Fig. 5 gives V_g/V_{ca} as 2.30 and so $V_{g1} = 23.5$ V. The second approximation gives $V_g/V_{g1} = -0.88$ but makes a negligible difference to the values of R_i, G_t, and N. The corrected value of K is 0.98. Hence $V_g/V_{ca} = 2.35$ and $V_{g1} = 24.3$ V. Similarly for dynamic resistances of 5,000 Ω and 2,500 Ω the values of V_{g1} are 14.9 V and 9.0 V. Since the ratio R_g/X_g is 63 the possible error in V_{g0} from this cause is less than 0.5% (Fig. 4).

An experimental arrangement was set up having the constants specified above and the oscillation amplitude was measured for the three cases. The values found were 23.8, 14.9, and 8.2 volts. It should be pointed out that this example is particularly unfavourable to the theory, as this type of valve, because of the unusually small length-to-diameter ratio of the electrodes, shows a considerable 'tail' in the anode-current grid-voltage characteristic; i.e., the actual relation differs considerably from the assumed three-halves law for values of i_a less than about 25% of I_0.

As a result of this divergence the anode current is always greater than the theoretical value, and may be considered to be the sum of the theoretical current and an extra current. From the integral given in the preceding Section for the value of I_{a1} it can be seen that when V_{g1} is large the angle of flow, β, is small. The extra current then flows mainly when $\cos\theta$ is positive, and the true value of V_{g1} is therefore greater than the theoretical value, but the difference is not large because, for large values of V_{g1}, the theoretical current is much greater than the extra current.

When V_{g1} is small most of the extra current flows when $\cos\theta$ is negative, and is relatively greater, both in magnitude and duration, than when V_{g1} is large. I_{a1} and thus V_{g1} is then less than the theoretical value, and the fractional error should be greater than for large values of V_{g1}. This is borne out in the example above by the comparatively large error of 10% at the smallest value of V_{g1}. At the largest value the error is of opposite sign to that expected, but since the error is small this discrepancy may reasonably be attributed to experimental errors and inaccuracies in the computation.

Better agreement between theory and experiment would be expected with valves of normal construction.

(To be concluded)

PHYSICAL SOCIETY'S EXHIBITION

Scientific Instruments and Apparatus

At this exhibition, held at Imperial College, London, from 5th to 8th April, there was a continuation of the policy, introduced last year, of asking exhibitors to exclude apparatus designed mainly for radio and other engineers. Any discouragement which readers of this journal might see in such a request was again more apparent than real, for the requirements of physicists are increasingly inseparable from those of radio and electronic engineers, so that there was as much as ever to interest the latter. In fact, even ignoring apparatus that had been seen anywhere before, and severely condensing descriptions of new items, it will not be possible to refer to all of it.

Last year it was noted that the classification of exhibitors into Trade and Research sections was less clearly justified than hitherto. This year the division was abolished entirely; instead, the individual exhibits were marked in the catalogue to show which were in production. This change reflected the encouraging tendency for manufacture and research to proceed together.

In spite of complaints that have been made in the past about the organization of the exhibition, the stands were more closely crowded than ever, to the great discomfort of both exhibitors and visitors. The fact that in these difficult circumstances the exhibitors' staffs maintained such a high standard of technical information and helpfulness was not only commendable in itself but set an example to other technical exhibitions.

Meters

The design of valveless instruments continues basically unchanged, but an interesting development was the vacuum-enclosed electrostatic voltmeter shown by Metrovick. The vacuum spacing enables the safe voltage gradient to be increased ten-fold and the deflecting force 100-fold, leading to a remarkably robust construction and freedom from troubles due to dust, moisture, convection, etc. The pointer difficulty is overcome by optical deflection. Another reflecting instrument in which the disadvantages that used to be associated with this type were notably absent was the Cambridge Instrument Co's dead-beat S.M.I. galvanometer, with a period of only 0.1 sec. The same firm's celebrated Unipivot instruments appeared in new moulded cases of modern design. External and other detail improvements were also to be seen on most of the stands showing meters. The Salford "Minitest" was notable for its small size, 4in × 3in × 1in, and for its neat edge-operated switches.

A number of new valve voltmeters were shown, progress being chiefly in the direction of greater sensitivity, low input admittance, and freedom from zero instability. Some of them, such as the Doran electrometer valve voltmeter, with grid current less than 5×10^{-12} A, were sufficiently good in these respects to be suitable for pH measurement. The usual type of instrument for normal use, of which the W. G. Pye and Avo were examples, includes a twin triode with meter connected between cathodes, a probe head, and stabilized power from an a.c. supply. The B.T-H. d.c. millivoltmeter, with ranges giving full-scale deflections from 5 mV to 1 V, works on the chopper method with a.c. amplification and has an input resistance exceeding 100 MΩ. The Edwards electronic microammeter, on the other hand, contains a stable d.c. amplifier, and the ranges are from 0.05 to 500 μA f.s.d.

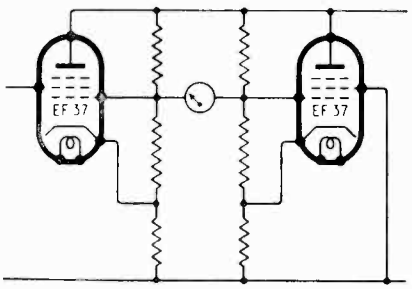

Fig. 1. *Circuit of zero stabilizer used in Avo Type W electronic test-meter.*

The monopoly of valves in the r.f. meter field was challenged last year by the Furzehill germanium 'valve' voltmeter: this year a significant innovation was the Airmec millivoltmeter Type 762, for use up to 500 Mc/s, in which a silicon-crystal rectifier is followed by a magnetic amplifier.

The enormous range of measurement possible with the Avo electronic test-meter has been carried a considerable stage further in Type W, made to a Service specification, which provides no fewer than 80 ranges. The full-scale voltages, for example, range from 0.1 to 10,000. To overcome zero instability due to valve contact-potential fluctuations, the basic circuit shown in Fig. 1 is used in place of the customary twin-triode system. The well-known Taylor multi-range meters now include an electronic test-meter (Model 170A), covering all general requirements in 40 ranges.

Cathode-Ray Equipment

In the British Physical Laboratories' Voltascope, a valve voltmeter is combined with a cathode-ray oscilloscope in which useful features are the balanced d.c. amplifiers for both x and y plates, giving instantaneous shifts, and sweep expansion up to 5 times screen diameter. Another compact general-purpose oscilloscope was the Panax Model 2c. A notable example of miniaturization applied to oscilloscopes was the Airmec Model 721, with alternative separate power units—Type A for 6 V d.c. or the usual a.c. mains supplies, or Type B for a.c. mains only and capable of running up to five oscilloscopes at once.

At the other end of the scale were the very elaborate equipments by Avimo and Cinema-Television, capable

of recording or displaying a number of traces simultaneously.

The Dawe Type 709A has been designed mainly for transient work, for example in nuclear physics and radar. A self-contained delay line enables the signal to be recorded after the start of the time base, triggered by itself. Applicable to transients of extremely short duration was the ultra-high-speed instrument shown by W. Nethercot on the British Electrical Research Association stand. Using the G.E.C. 908 BCC tube with 10 kV and a f/1.0 lens, writing speeds up to 20,000 km/sec can be recorded as single transients, with a resolution of 0.001 μsec.

Standards and Bridges

Some interesting additions to the Sullivan range of variable air capacitors were to be seen. In one, a combination vane assembly includes two rotors, one of them continuously rotatable and the other moving in 10 steps. Each step brings in a capacitance equal to that of the continuously-variable section, thereby providing a decade extension and giving a scale accuracy 10 times that of an ordinary variable capacitor of the same range. No extra loss is introduced by the decade, for it is mounted on the same solid dielectric (silica) as the variable section. An ingenious shaping of the vanes excludes errors due to any slight variations in the step locating of the decade section. The laboratory grade of air capacitor has been redesigned with quartz mountings and other detail improvements; and a miniature series has been introduced, providing the Sullivan smoothness of rotation and stability of calibration in a much smaller bulk than hitherto.

The W. G. Pye Type 940067 variable capacitor, designed primarily for the Pye r.f. bridge, is notable for the mechanical precision of its 50 : 1 worm gear, as may be judged from the fact that a change of 0.1 pF can be read in the total range of 600 pF over which variation is accurately linear. The bridge (Type 940073) measures admittance over the frequency range 0.1–20 Mc/s, and employs inductively-coupled ratio arms.

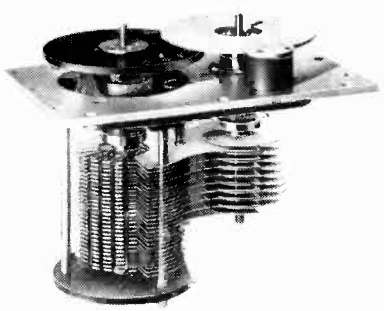

Sullivan-Griffiths variable air-capacitor with decade extension.

The same principle has been much used in the Wayne-Kerr r.f. bridges, capable of balanced or unbalanced measurements of admittance up to 100 Mc/s. Above this it is difficult to achieve sufficiently low leakage inductance in the ratio arms, but an experimental model was shown for use up to 200 Mc/s. An alternative solution was shown by the B.B.C. for use from 10 to 250 Mc/s, employing capacitance ratio arms; but perhaps its most interesting feature is the device whereby the resistance arms are varied without changing their shape or reactance. They are thermistors, varied by superimposed direct current, their resistances being determined in situ by subsidiary bridge measurement.

Working at the comparatively low radio frequency of 23.88 kc/s, the B.P.L. Model LB.320 is a modified Maxwell bridge invented by F. Clifford of the G.P.O. to give direct readings of coupling coefficient k as well as L and Q. This is done by taking a second reading with the coupled coil short-circuited.

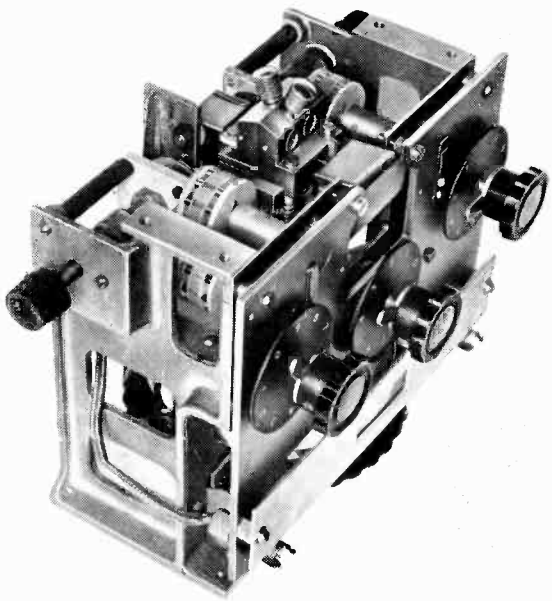

50–500 Mc/s bridge, showing construction typical of Wayne-Kerr v.h.f. instruments.

The Dawe Q-Meter Type 622A works on the usual principle, over a frequency range of 50 kc/s to 75 Mc/s, but the Marconi Instruments Type TF.886, for 15 to 170 Mc/s, is unusual in using an inductive step-down from the source to the resonant circuit, the source and resonance output being balanced against one another by a control calibrated in Q. An application of the Q-meter method to measure something quite different—the salinity of solutions—was demonstrated by the Admiralty Experimental Establishments. The measurement depends on the loss introduced by a column of brine capacitively coupled to a 12-Mc/s circuit. Its advantage is the absence of direct contact between electrodes and solution. Normal Q-meter techniques are not applicable at 3,000 Mc/s, but Wayne-Kerr showed a decrement method of measuring the Q of echo boxes in that band.

Electronic devices have greatly extended the choice of detectors for bridges and kindred apparatus. One of a number of examples on view was the Airmec heterodyne bridge detector, covering a frequency range of 9–750 kc/s and giving a readable meter deflection for 5μV input and an audible note for 1μV. The intermediate frequency is 1 kc/s. An alternative use for this instrument is as a wave analyzer.

Oscillators

The choice of oscillators for bridges and other purposes has also been extended. Although the tendency in the a.f. range is still for resistance-capacitance types to predominate, several new beat-frequency types were shown. Of these, the Furzehill Type 2232, 20 c/s–20 kc/s, employs eddy-current tuning.

The RC-type of oscillator was represented by: the B.P.L. Model LO.63-A, for which a frequency stability of 1 in 5000 is claimed; the Muirhead D-330-B, recently improved by lining up the circuits so that a single frequency scale holds accurately on all three ranges; and a Sullivan model which is exceptional in using the phase-shift network instead of the Wien bridge, and in stabilizing amplitude by applying to the suppressor-grid of the maintaining valve a bias derived by rectifying the oscillation.

Interesting for its mechanical design was the Wayne-Kerr v.f. oscillator, of the LC-type, with a frequency range from 7 kc/s to 7 Mc/s. The appropriate direct-reading frequency scale, marked on a vertical roller, is automatically brought into view by operation of the range switch; and access to the valves is instantly available by pulling out a panel on the front of the instrument.

Another interesting type of oscillator was the Television Sweep shown by Marconi Instruments. This generates a carrier wave, variable up to about 100 Mc/s, which can be mechanically frequency-modulated at 500 c/s over several Mc/s. The ease with which the matching and electrical length of lines and the frequency characteristics of television aerials can be investigated by this oscillator in conjunction with an oscilloscope was convincingly demonstrated. Pulses of adjustable amplitude (0–75 V), width (1, 10, and 100 μsec), and repetition rate (1–10,000 per sec) are provided by the Dawe Type 412 Pulse Generator, designed primarily for nuclear physics but obviously useful in the television laboratory. Plessey showed a reflex-klystron source of centimetre-waves, calibrated in frequency over a 1.5 : 1 range (with crystal check) and in amplitude using a piston attenuator.

British Physical Laboratories precision frequency meter, 10–110 c/s.

Power Supplies

The large variations in voltage and frequency of public electricity supplies during recent years has necessitated counter-measures in laboratories which rely on such supplies. In many items of mains-driven apparatus special attention has been given to this, usually in some form of voltage stabilization. Separate

Cinema-Television universal valve tester in which any desired valve characteristics can be displayed on a calibrated c.r. tube.

stabilized power units were again shown by a number of makers, including Dynatron with a unit (Type P.200) adjustable from 200 to 4000 V in four ranges. But where much voltage-sensitive equipment is used it is more convenient and may be more economical to stabilize the a.c. supply in bulk, and automatic voltage-regulating units were shown by Berco, Gresham, and Zenith, comprising regulating transformers adjusted by motors controlled by a relay working on the difference between input and output voltage. Berco units have been designed for single-phase and for 3-phase supplies. Up to 6 kVA single phase and 9.5 kVA 3-phase, the

whole power is handled by the variable transformer; but control of up to 75 kVA can be arranged by using the regulating transformer as a booster to adjust only the variable part of the whole voltage.

Low-voltage d.c. power units to replace batteries have hitherto not been readily available, but one shown by Labgear provides up to 12 V at 5 A with only 0.1% residual ripple.

Miscellaneous Apparatus

One of the outstanding features of the exhibition was the large amount and variety of apparatus for counting, measuring time intervals, and computing. Much of this equipment employs techniques familiar to radio engineers, or is directly applicable to radio research; but space does not permit even a bare mention of the many exhibits.

Counters were shown applied to batching of manufactured products, the determination of engine speed, the nimbler tasks of atomic research and radioactivity, and as essential parts of digital computers. The greater part of the Elliott Bros. stand was devoted to apparatus for the manipulation of large quantities of data; the exhibits included a photo-electric curve follower, a binary arithmetic calculator, and a simultaneous-equation solver, with a capacity of 12 unknowns. The electrical analogue type of computer was represented in the exhibition by the Sperry Electronic Simulator for solving differential equations encountered in servo design. A graphical harmonic analyzer of the planimeter type, for determining the sine and cosine terms of the first eight harmonics, was shown by W. F. Stanley, along with integrators and other instruments of similar construction.

A.F. wave analyzers of the heterodyne type were shown by Dawe (Type 705A) and Wayne-Kerr (Type A.201); and the novel method of analysis demonstrated some years ago by D. M. Tombs, in which a resonant circuit with variable negative resistance, coupled to the source of the waveform, is tuned successively to each harmonic frequency, appeared in a more highly-developed form.

Apparatus for measuring frequency and time included: a crystal-controlled frequency standard giving both sinusoidal and pulse outputs at 0.1, 1, 10, 100 and 1000 kc/s, with a synchronous clock for long-period comparison; a direct-reading frequency meter and tachometer for frequencies up to 20 kc/s, operating on inputs of any waveform and as little as 0.1 V amplitude; a time-interval meter of the capacitor-discharge-time type reading from 1 msec to 20 sec—all the foregoing by Airmec—and a 1-kc/s temperature-controlled crystal standard of 1 in 10^6 stability and a precision mains-frequency meter, both by B.P.L. This frequency meter, range 10–110 c/s, which is also independent of amplitude and waveform, incorporates a Carpenter relay, and the reading is indicated directly on decade dials in steps of 0.1 c/s. The application of the stroboscope to show musical pitch directly was demonstrated by Dawe with a rotating cylinder marked with alternate black and white segments, and illuminated by a neon lamp energized by the output of an audio amplifier at the sound frequencies being measured.

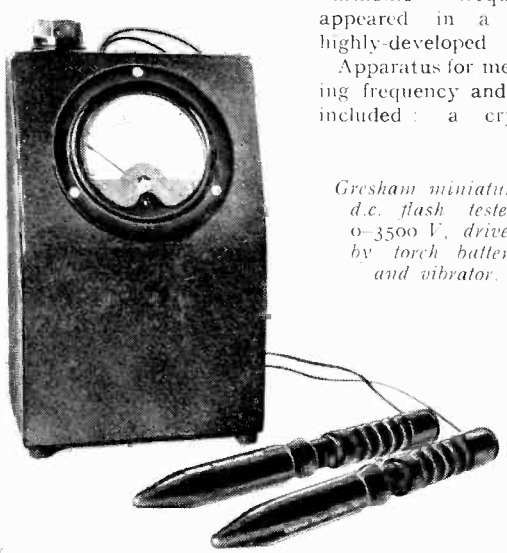

Gresham miniature d.c. flash tester, 0–3500 V, driven by torch battery and vibrator.

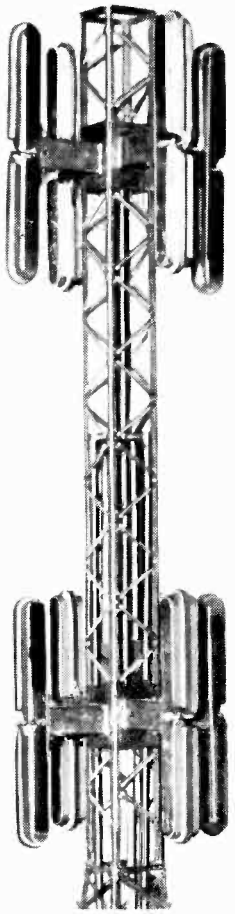

Scale model of top half of Sutton Coldfield television aerial, used for B.B.C.-Marconi design testing.

An elaborate acoustic measuring equipment was demonstrated by B.T-H., comprising a generator of steady, warbled or pulsed tone, with an amplifier, a microphone with its amplifiers, a high-speed level recorder, and an oscilloscope. With this set-up it is possible to measure frequency characteristics, reverberation times and echo patterns. The same apparatus with a limiting amplifier was used to show delayed resonance characteristics of loudspeakers, as investigated by Shorter of the B.B.C. and illustrated by a 3-dimensional model on their stand.

B.T-H. also exhibited a mains-driven noise meter with a very high-gain amplifier in which special precautions had been taken to minimize internal noise and permit noise as low as 15 phons to be measured, weighting networks to simulate ear characteristics at three levels, and peak and mean meters.

Last year magnetic amplifiers first appeared

prominently; this year attention was directed to their applications. These included amplification in a sensitive r.f. meter (Airmec), super-sensitive temperature measurement by ordinary milliammeters (Electro Methods), operation of temperature recorders (Everett Edgcumbe), intrinsically-safe level indication of inflammable liquids (Electro Methods), and industrial counters (Elliott Bros.). The long time constant of the magnetic amplifier has hitherto confined its applications to frequencies seldom above 10 c/s; but by the use of Ferroxcube magnetic material (shown last year) and the high carrier frequency of 100 kc/s, Mullard were able to demonstrate amplification of musical frequencies.

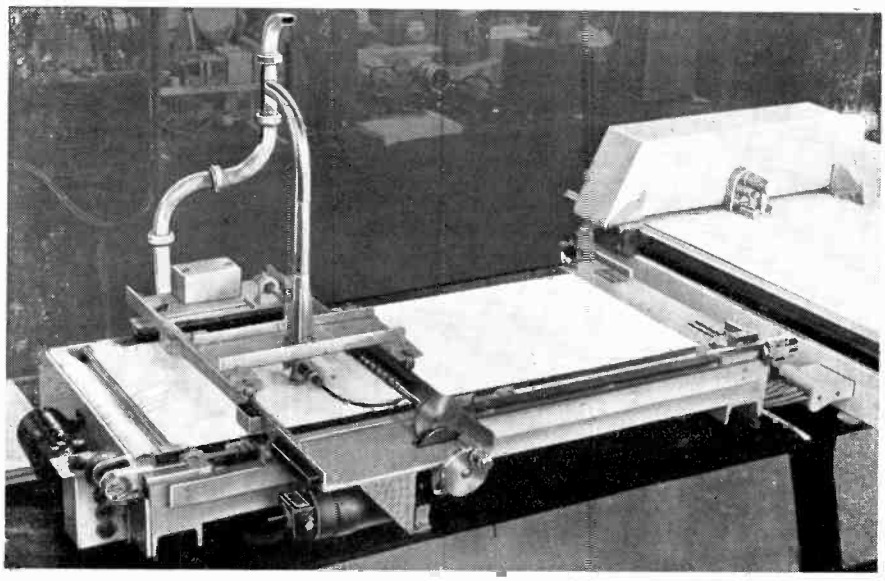

Elliott automatic phase-front plotter for microwave radiators.

In half an hour spent with the Cinema-Television valve tester one could learn more about valve characteristics than by days (it would hardly be an exaggeration to say a lifetime !) without it. Current/voltage curves for any electrode at ten different grid potentials are displayed simultaneously on a c.r.t. screen, and the effects of varying the potentials of any of the other electrodes can be studied. Slope can be measured by comparison with a variable linear resistance line. A system of push-button switches enables any combination of supplies to any valve to be set up in a few seconds; and both valve and apparatus are fully protected against overloads.

Demonstration of the T.C.C. Discharge Detector showed how voids in the dielectric of high-voltage capacitors, which would cause premature failure, are revealed by visual and aural signals resulting from ionization. A somewhat similar principle is applied to a variety of leakage tests in the Airmec Ionization Voltage Tester. The Gresham Miniature D.C. Insulation Flash Tester attracted attention by its small size, safety, and portability. Its power unit is a torch battery, generating up to 3500 V by a vibrator.

Hitherto the cost of making Schmidt correction lenses for television and radar in glass has been excessive; but specimens in two different sizes on the Optical Works stand had been made by a new process which has brought the cost of a Schmidt projector to a more reasonable figure.

Research

No fewer than six establishments of the Ministry of Supply exhibited. Among the items of radio interest were: a substantially achromatic metallic delay lens for microwave radiators, in which zinc strips were suspended normal to the planes of polarization and propagation; a display showing the construction and use of klystrons and associated plumbing for work with 7–12-mm waves; and apparatus for measuring acoustic resistance and reactance in terms of electrical standards. The last of these utilized a Wigan-Muirhead a.c. potentiometer of novel design, in which in-phase and quadrature components were obtainable with precision over an exceptional range of frequency.

Some most elegant demonstrations were given of the far-reaching possibilities of an extremely simple mechanical device—a spring consisting of a metal strip with its ends pushed towards one another and held at angles so as to form it into a shape resembling a sine curve. The stiffness of the centre of the strip, in the direction at right angles to a line joining its ends, can be varied continuously from positive to negative values. In one application, relay contact pressure was shown to increase right up to the instant of a rapid break.

The 1:7.5 scale model of the Sutton Coldfield television aerial, which was used in tests carried out at correspondingly higher frequencies, and a diagram of a method used for obtaining vertical polar diagrams of medium-wave aerials, were shown by the B.B.C. Elliot Bros. demonstrated automatic plotting of the phase front of microwaves in the region of a radiator. An electrolytic analogue for the study of electrical networks was shown by members of the Imperial College staff.

A development of great technological interest was the soldering of aluminium demonstrated by Mullard. Tin/zinc solder is used, and no flux; the oxide film is broken down mechanically by vibrating the iron at ultrasonic frequency by magnetostriction.

Valves and Cathode-Ray Tubes

Use of the travelling-wave tube shown last year by Standard Telephones has now been extended to the 3-cm band. The same firm showed a 6–7 cm klystron giving a c.w. output of 5 W with an input of 50 W.

This waveband has now been invaded by a triode—the G.E.C. E.1771, an experimental disk-seal type.

The Mullard range of subminiature valves has been greatly enlarged by 11 mains types in addition to electrometer triodes and tetrodes. What might almost be called a sub-subminiature diode, only $\frac{1}{8}$-in diameter, was shown at various stages of manufacture by Standard Telephones.

Another new Mullard valve was the EQ40 nonode, with two gating control grids, for use as a combined limiter-discriminator in f.m. reception.

The Ediswan 9-stage electron-multiplier is now made with a quartz envelope to extend the range of transmitted light at the ultra-violet end. Their 20A2 xenon-filled thyratron is notable for its high mean I_k rating—125 mA.

Amplification by transistors, or germanium-crystal triodes, was demonstrated by B.T-H and Standard Telephones. These devices, smaller even than subminiature valves, are biased to about + 0.5 V on the input electrode and of the order of − 50 V on the output.

A number of specialized cathode-ray tubes were shown by G.E.C.: the 908 BCC high-speed type already mentioned; the 1608 ABCA, a similar tube with post-deflector acceleration, giving three times the sensitivity; the 2211.BXA 9-in electrostatic precision television monitor; the 1693.HKM monoscope with various test patterns; and a 40-contact c.r.t. switch operable at television carrier frequencies.

Materials

The increasing versatility of bakelite plastics in scientific instruments was shown on the Bakelite stand. Tufnol is an insulator with exceptional mechanical strength and durability, an aspect which was brought out in a radio-component life-testing machine with cams of that material

Synthetic production of two types of piezo-electric crystal were illustrated by G.E.C.—synthetic quartz as a substitute for the natural product in times of scarcity, and ethylene diamine tartrate, preferable to quartz in selective filters.

The usefulness of the Murex sintered-powder method of permanent-magnet production has been increased by the introduction of Alcomax II powder, giving a higher flux density, and the technique of composite iron-alnico bodies. The gap and locating holes, in the iron portion, can be accurately machined, while obtaining the advantage of a continuous magnet. Magnetic-shunt alloys produced by Telcon have temperature coefficients of permeability which enable them to be applied to moving-coil meters in such a way as to compensate for temperature errors due to the conductors. In addition to magnetic materials previously noted, Plessey showed samples of Caslam, consisting of flake-iron particles pressed into the desired shape for a.c. cores, as an economical alternative to laminated stampings.

For soldering metal structures that have to resist high temperatures, the Mond Nickel Co. showed a palladium alloy with which joints can be made capable of taking a sheer load of 6 ton/in^2 at 600° C.

A great variety of special materials were shown by Johnson, Matthey & Co., of which one of the most potentially important was contact bi-metal, in which a facing of electrical contact metal is bonded to a copper-alloy backing. This technique offers a number of advantages over rivet contacts. Precious-metal contacts for precision instruments were also among the exhibits of Electro Methods.

CORRESPONDENCE

Letters to the Editor on technical subjects are always welcome. In publishing such communications the Editors do not necessarily endorse any technical or general statements which they may contain.

Negative Feedback Amplifiers

SIR,—In the article in your February issue, in which C. F. Brockelsby describes a method for designing feedback amplifiers with the maximally flat overall-response, he goes on to claim that 'a substantially flat response over the maximum possible frequency band can be obtained with any amount of feedback,' and that, in contrast to the methods described by Terman and other writers 'giving a *maximum* value for the feedback which can be applied without self-oscillation,' in his method 'there is no limit to the amount of feedback that can be applied.'

This, as it stands, is misleading.

Brockelsby deduces from the well-known formula for the external gain of a feedback amplifier

$$A_z = \frac{A}{1 + A\beta}$$

the conditions for a 'maximally flat' response in a 3-stage amplifier, and points out that such an amplifier is necessarily stable: most feedback amplifiers have humps in their external amplification characteristics, and oscillation occurs when these humps become infinite. The condition for maximal flatness is that two stages should be identical and broad-band, while one stage is narrow-band. The ratio of the bandwidths increases with the feed-back factor, being 20 : 1 for 20 db, and 55 : 1 for 40 db. The effective feedback is $(1 + A\beta)$, and this falls away outside the band of the narrow stage. The amplifier has therefore got a narrow band of high feedback, and outside it a flat external gain characteristic with a feedback factor falling to less than unity at the edge of the band.

If it is necessary to build an amplifier with effective feedback at the lower end of the pass-band only, and it is impossible to remove the humps in the characteristic by filters outside the loop, then this is an excellent way of designing it. More often, however, uniform feedback over the pass-band is required, and as the humps lie well outside it, they are not difficult to deal with. When not only the maximum feedback obtainable but the band over which it is actually available is considered, it becomes clear that Mr. Brockelsby's design is inefficient, and his claim that there is no limit to the amount of feedback which can be obtained means only that by making the effective band infinitely narrow, the feedback factor over it may be made infinitely great. The factor limiting the (effective feedback) × (band-

width) product is that the rapid increase of the bandwidth of the broad stages as the feedback factor is increased results in a point being reached at which the gain of the circuit is inadequate to provide the amount of feedback required.

The reasons why the optimum design for a three-stage feedback amplifier has two narrow stages and one broad one have been fully analysed by Bode*, and this is not the place to repeat them.

I have calculated the amounts of feedback obtainable in two typical cases by the two methods. With valves having a slope of 5 mA/V and interstage capacitances of 20 pF, I have taken for the first case a bandwidth of 1 Mc/s and an external gain of 20 db and for the second a bandwidth of 100 kc/s and an external gain of 40 db. Bode's method gives feedbacks of 52 db and 67 db respectively while Brockelsby's gives 25 db and 42 db.

T. S. McLeod.

Standard Telecommunication Laboratories Limited, Enfield.

Non-linear Effects in Ring Modulators

Sir,—The operation of rectifier modulators is usually discussed by assuming that the signal voltage is small compared to the carrier voltage. It is well known that for larger signals the modulator acts as a limiter and this is often considered desirable for channel modulators in carrier-telephone systems. In group modulators, on the contrary, too large signals cause prejudicial intermodulation. None of these effects seems to have been calculated theoretically for ideal ring modulators and the purpose of this note is to show how simple and practical expressions can be obtained.

For small signal voltages, the passing or blocking condition of the rectifier only depends on the sign of the carrier voltage

$$v_c = V_c \cos 2\pi Ft$$

and this leads to the Fourier series†

$$\text{sign} \cos 2\pi Ft = \frac{4}{\pi}(\cos 2\pi Ft - \frac{1}{3}\cos 6\pi Ft + \ldots).$$

For arbitrary values of the signal voltage $v_s = V_s \cos 2\pi ft$, the conditions of the four rectifiers depend on the signs of the four expressions contained in $\pm v_c \pm v_s$ respectively, and the instantaneous output voltage is

$$v = \frac{1}{2} v_s [\text{sign}\,(v_c + v_s) + \text{sign}\,(v_c - v_s)] + \frac{1}{2} v_c [\text{sign}\,(v_c + v_s) - \text{sign}\,(v_c - v_s)] \quad \ldots \quad (1)$$

The amplitudes of individual modulation products are deduced from (1) by expanding

$$\text{sign}\,(v_c + v_s) = \text{sign}\,(\cos 2\pi Ft + k \cos 2\pi ft)$$

where k stands for the ratio V_s/V_c, into a double Fourier series. The Fourier coefficients have been expressed by W. R. Bennett in terms of hypergeometric functions (*Bell Syst. tech. J.*, Vol. 12, p. 228, April 1933 and Vol. 14, p. 322, April 1935). Combining the contributions of the four terms of (1) which correspond to the same frequency and using recurrence formulae for the hypergeometric functions the amplitude V_{mn} of the component of frequency $mF \pm nf$ is found to be

$$V_{mn}/V_c = \frac{k^n \Gamma\left(\frac{m+n-1}{2}\right)}{\pi \Gamma(n+1)\,\Gamma\left(\frac{m-n+3}{2}\right)} \times F\left(\frac{m+n-1}{2}, \frac{n-m+1}{2}, n+1;\ k^2\right).$$

Only products corresponding to odd values of m and n exist, due to the balance of the modulator. The attached curves show how the level of the lowest products varies with signal to carrier ratio.

The dominant products for small signal voltages are $mF \pm f$ and vary linearly with the signal; for large signal voltages, the dominant products $F \pm nf$ vary linearly with the carrier level. Curve V_{11} gives the limitation characteristic; the amplitude V_{11} is easily expressed in terms of complete elliptic integrals of the first and second kind with modulus k:

$$V_{11}/V_c = \frac{8}{3\pi^2 k}[(k^2+1)\,E + (k^2-1)\,K]$$

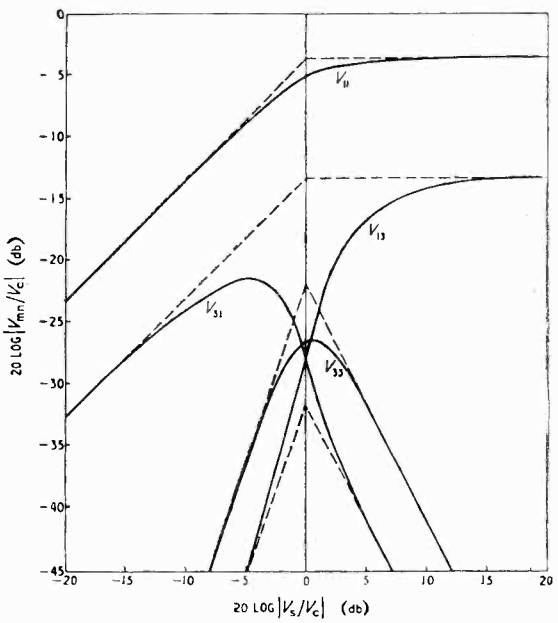

For small signal voltages, the non-linear distortion of the modulator is characterized by the level of the component $F \pm 3f$ relative to the useful sideband $F \pm f$. This distortion level is approximately

$$20 \log \frac{24}{k^2} = 40 \log |V_c/V_s| + 27.6 \text{ db}.$$

Similar results hold for ideal bridge modulators but the levels of all products are decreased by 6 db; additional products with m even and n odd, including input leak, also appear in that case.

V. Belevitch.

Brussels, Belgium.

* H. W. Bode. "Network Analysis and Feed-back Amplifier Design," (MacMillan).

† Sign x = the signature of x and is defined as sign $x = +1$ when x is positive, sign $x = 0$ when $x = 0$, and sign $x = -1$ when x is negative.

NATIONAL PHYSICAL LABORATORY

The N.P.L. 'Open Day' is being held this year on Thursday, 26th May from 2.30—6 p.m. for representatives of industrial organizations, and on Friday, 27th May for members of university staffs and Government departments.

Accredited representatives of industrial organizations who wish to visit the Laboratory should apply to the Director, National Physical Laboratory, Teddington, Middlesex, not later than 14th May.

WIRELESS PATENTS

A Summary of Recently Accepted Specifications

The following abstracts are prepared, with the permission of the Controller of H.M. Stationery Office, from Specifications obtainable at the Patent Office, 25, Southampton Buildings, London, W.C.2, price 2/- each.

AERIALS AND AERIAL SYSTEMS

604 008.—Mat or grid type of aerial, and means for supporting it under the running-board or chassis of a motor-car.

E. St. J. Chesney. Application date 20th November, 1945.

604 582.—Directive aerial of the wave type, which is coupled to a grounded-grid oscillator valve in such a way as to provide a feedback circuit through the correct value of surge impedance.

Standard Telephones and Cables Ltd. (assignees of G. T. Royden). Convention date (U.S.A.) 9th April, 1945.

604 772.—Rotatable aerial system for direction-finding, comprising three waveguide horns, two arranged symmetrically about the major axis, while the third is mounted in that axis.

Cie Generale de Telegraphie Sans Fil. Convention date (France) 7th July, 1944.

DIRECTIONAL AND NAVIGATIONAL SYSTEMS

603 727.—Navigational indicator for correlating the readings of a track reference dial and a magnetic compass, with a radio direction-finder and a fixed reference or lubber-line.

Bendix Aviation Corporation. Convention date (U.S.A.) 31st October, 1944.

603 769.—Radiolocation apparatus of the anti-collision type wherein provision is made for reversing the sense of echo-signals coming from objects at a distance exceeding say two miles, in order to simplify the critical indications.

Marconi's W.T. Co. Ltd., and R. J. Kemp. Application date 14th December, 1945.

603 901.—Circuit arrangement for maintaining a correct threshold-bias on the responder equipment used to identify different aeroplanes when these come under radar observation.

Ferranti Ltd., M. K. Taylor and F. C. Williams. Application date 5th November, 1945.

604 096.—Synchronized switching system for a direction-finder using a number of fixed aerials with overlapping directional field patterns.

Standard Telephones and Cables Ltd. (assignees of N. Marchand). Convention date (U.S.A.) 25th November, 1944.

604 227.—Direction finder coupled to aerials of the Adcock type through separate amplifying channels, each of which is provided with an independent automatic gain-control.

Western Electric Co. Inc. Convention date (U.S.A.) 17th February, 1942.

604 239.—Control circuit for the oscillator valve of the responder equipment used to distinguish different aeroplanes when under radar observation.

Ferranti Ltd., M. K. Taylor and F. C. Williams. Application date 5th November, 1945.

604 445.—Navigational system utilizing a chain of beacons for radiating guiding beams on different frequencies and intermediate marker-beacons which automatically change the tuning of the mobile receiver from point to point.

Standard Telephones and Cables Ltd. (assignees of E. M. Deloraine and P. R. Adams). Convention date (U.S.A.) 5th May, 1944.

604 462.—Phase-adjusting device for automatically stabilizing the direction of the median line in radio-navigational beacons of the overlapping-beam type.

W. J. O'Brien. Convention date (U.S.A.) 13th April, 1942.

RECEIVING CIRCUITS AND APPARATUS

604 255.—Voltage-control system for selecting the optimum signal at the central point of an anti-fading arrangement of spaced aerials.

Philips Lamps Ltd. Convention date (Netherlands) 31st July, 1940.

604 652.—H.F. transformer coupling, particularly for a push-pull amplifier in which the primary consists of two transmission lines connected in parallel, and the secondary is another transmission line movable about a pivot.

Standard Telephones and Cables Ltd. (assignees of H. Romander and B. V. Thompson). Convention date (U.S.A.) 28th March, 1945.

CONSTRUCTION OF ELECTRONIC-DISCHARGE DEVICES

602 464.—High-powered electron-discharge tube of the hollow-resonator type, for generating short-wave oscillations, or for modulating them in frequency or amplitude.

Marconi's W.T. Co. Ltd. (assignees of F. H. Kroger). Convention date (U.S.A.) 27th March, 1940.

SUBSIDIARY APPARATUS AND MATERIALS

602 140.—Process for producing an alloy of silicon and boron having high sensitivity as a rectifier of centimetre waves.

Western Electric Co. Inc. Convention date (U.S.A.) 20th July, 1944.

602 145.—Electro-mechanical vibrator, of the tuning-fork type, in which there is at least one displacement-free and rotation-free point of support.

"Patelhold" Patentverwertungs &c A.G. Convention date (Switzerland) 13th December, 1944.

603 169.—Traffic-control system in which the reflection of a centimetre-wave radio beam is used for the automatic operation of 'right-of-way' signals.

Automatic Signal Corporation. Convention date (U.S.A.) 17th May, 1944.

603 299.—Chassis arrangement in which a series of apertured cross-members are spaced along a pair of parallel rails in order to support the various circuit-components used in telecommunication.

Philips Lamps and K. E. Latimer. Application date 29th May, 1945.

603 454.—Push-pull oscillation generator designed to ensure the safe-handling of high-frequency appliances used for industrial or medical purposes.

H. W. K. Jennings (communicated by E. Mittelmann). Application date 7th August, 1945.